

Statistical Roughness-Informed Machine Unlearning

Mohammad Partohaghīghī^a, Roummel Marcia^b, Bruce J. West^c, YangQuan Chen^d

^a*Electrical Engineering and Computer Science, University of California, Merced, CA 95343, USA*

^b*Department of Applied Mathematics, University of California, Merced, CA 95343, USA*

^c*Department of Innovation and Research, North Carolina State University, Raleigh, NC, USA*

^d*Mechatronics, Embedded Systems and Automation (MESA) Lab, Department of Mechanical Engineering, School of Engineering, University of California, Merced, CA 95343, USA*

Abstract

Machine unlearning aims to remove the influence of a designated forget set from a trained model while preserving utility on the retained data. In modern deep networks, approximate unlearning frequently fails under large or adversarial deletions due to pronounced layer-wise heterogeneity: some layers exhibit stable, well-regularized representations while others are brittle, undertrained, or overfit, so naive update allocation can trigger catastrophic forgetting or unstable dynamics. We propose Statistical-Roughness Adaptive Gradient Unlearning (SRAGU), a mechanism-first unlearning algorithm that reallocates unlearning updates using layer-wise statistical roughness operationalized via heavy-tailed spectral diagnostics of layer weight matrices. Starting from an Adaptive Gradient Unlearning (AGU) sensitivity signal computed on the forget set, SRAGU estimates a WeightWatcher-style heavy-tailed exponent for each layer, maps it to a bounded spectral stability weight, and uses this stability signal to spectrally reweight the AGU sensitivities before applying the same minibatch update form. This concentrates unlearning motion in spectrally stable layers while damping updates in unstable or overfit layers, improving stability under hard deletions. We evaluate unlearning via behavioral alignment to a gold retrained reference model trained from scratch on the retained data, using empirical prediction-divergence and KL-to-gold proxies on a forget-focused query set; we additionally report membership inference auditing as a complementary leakage signal, treating forget-set points as should-be-forgotten members during evaluation.

Keywords: Machine Unlearning, Heavy-Tailed Spectra, Layer-wise Stability, Statistical Roughness, Spectral Diagnostics, Right to Erasure

1. Introduction

Context and Motivation. Modern machine learning systems operate under continuous change: new data arrives, policies evolve, deployments are audited, and users or institutions may request that specific records no longer influence a model. This reality is reinforced by regulatory frameworks that formalize deletion and control rights over personal data, elevating *machine unlearning* from a niche security curiosity to a practical requirement in the model lifecycle [1, 2]. At a high level, unlearning seeks to remove the influence of designated training records while preserving utility on retained data, approximating the behavior of a model trained without the removed information [3, 4, 5].

Problem and Challenge. The ideal solution is conceptually simple: retrain from scratch on the retained data. In realistic settings, however, retraining is often prohibitively expensive due to repeated deletion requests, large-scale models, and production constraints. This gap has motivated a spectrum of efficient unlearning techniques, but efficiency alone is not enough: approximate unlearning can be unstable, degrade utility, or provide weak deletion fidelity under adversarial or high-impact forget requests [6, 7, 8, 9, 10]. Moreover, unlearning is tightly entangled with the broader problem of model leakage and memorization, where attackers may infer membership or extract training content, making robust removal mechanisms particularly important in sensitive domains [11, 12].

Prior Work Positioning. Early formulations framed unlearning as a system-level capability and explored transformations that support data removal [3]. Subsequent work developed deletion-efficient learning principles and scalable training frameworks such as sharding-and-slicing to enable partial retraining [4, 5]. For deep networks, practical approaches include selective forgetting and weight scrubbing [13, 14], update-caching and rollback-style strategies [15], decision-boundary shifting [16], and saliency-guided unlearning updates [17]. Recent research has also sharpened the understanding of what makes unlearning easy or hard, and proposed mechanisms that scale across unlearning desiderata and threat models [8, 9, 10]. Surveys provide structured taxonomies, metrics, and open problems across these families [24, 25, 26, 27].

Key Gap: Layer-wise Heterogeneity and Optimization Geometry.. A recurring practical obstacle is that deep networks are not uniform objects: layers can differ substantially in conditioning, stability, and how brittle their representations are under targeted updates. This heterogeneity interacts with optimization geometry, where sharpness, flatness, and basin structure have long been connected to stability and generalization behavior [21, 22, 23]. In the unlearning setting, an update rule that is globally sensible can still be locally destructive when it concentrates changes in fragile regions of the network. This motivates unlearning mechanisms that are not only sensitive to *which parameters matter* for forgetting, but also aware of *which layers can safely absorb* the required modifications.

Our Idea: SRAGU. This paper introduces Statistical-Roughness Adaptive Gradient Unlearning (SRAGU), a drop-in enhancement to the Adaptive Gradient Unlearning (AGU) baseline [18]. AGU prioritizes unlearning updates using sensitivity signals computed from the forget set, offering an efficient and appealing starting point. SRAGU retains this sensitivity-driven prioritization but modulates it using a layer-wise stability signal derived from heavy-tailed spectral diagnostics of weight matrices, inspired by empirical heavy-tailed phenomena in trained deep networks and their interpretation through random-matrix perspectives [19, 20]. Intuitively, SRAGU steers unlearning effort toward layers that appear spectrally stable and away from layers that exhibit signatures of brittleness or overfitting, improving robustness without adding expensive per-example instrumentation beyond the baseline workflow. This direction is also aligned with the broader trend of expanding unlearning beyond standard classification into modern generative and foundation-model settings, where targeted removal and behavior editing have become increasingly relevant [28, 29].

Contributions. We make the following contributions. First, we identify a concrete failure mode of sensitivity-driven unlearning that arises from layer-wise heterogeneity and optimization geometry, clarifying why efficient forgetting can become unstable. Second, we propose SRAGU, a stability-aware extension of AGU that uses heavy-tailed spectral diagnostics of layer weights to modulate unlearning updates. Third, we provide an implementation-ready methodology that integrates these diagnostics into unlearning with minimal disruption to standard training and evaluation pipelines. Finally, we position SRAGU within the broader unlearning landscape and connect its mechanism

to prior efficient unlearning paradigms, modern desiderata and hardness considerations, and known spectral/optimization phenomena [24, 25, 27, 9].

Roadmap. The remainder of the paper is organized as follows. Section 2 reviews machine unlearning and the AGU baseline in the context of representative unlearning families and evaluation desiderata. Section 3 presents SRAGU and Section 4 presents mechanistic analysis. Section 5 provides an empirical evaluation across deletion settings and baselines, and Section 6 concludes with limitations and future directions.

2. Methodology

The Roughness-informed machine unlearning framework enhances the Adaptive Gradient Unlearning (AGU) baseline by explicitly modeling geometric roughness in the loss surface and statistical roughness in layer-wise parameter distributions, enabling stable and reliable forgetting. This section formalizes the problem, reviews the AGU baseline, details its limitations, and presents the proposed SRAGU algorithms.

2.1. Problem Formulation

Assume a pre-trained model with parameters $\phi \in \mathbb{R}^n$, a forget subset $\mathcal{D}_{\text{forget}} = \{(u_i, v_i)\}_{i=1}^{|\mathcal{D}_{\text{forget}}|}$, and a retained data collection. The objective is to derive an adjusted parameter configuration ϕ' such that the model $F(\cdot; \phi')$ behaves as if trained exclusively on the retained data, i.e., without influence from $\mathcal{D}_{\text{forget}}$.

We quantify unlearning leakage via empirical alignment between the unlearned model and a gold retrained model (trained from scratch without $\mathcal{D}_{\text{forget}}$), following the prediction-divergence protocol used by AGU [18]. We define the empirical leakage proxy as:

$$\epsilon_{\text{pred}} = \max_{(x,y) \in \mathcal{D}_{\text{forget}}} \|p_{\text{unlearn}}(\cdot | x) - p_{\text{retrain}}(\cdot | x)\|_1, \quad (1)$$

where $p(\cdot | x)$ is the softmax predictive distribution. Smaller ϵ_{pred} indicates stronger forgetting (closer behavior to exact retraining) and reduced residual influence.

The process must also preserve performance on retained samples, quantified through accuracy or loss. The challenge lies in approximating ideal unlearning equivalent to complete retraining efficiently and robustly, particularly under large deletion ratios or adversarially chosen forget sets.

2.2. Baseline: Adaptive Gradient Unlearning (AGU)

AGU [18] is an efficient approximate unlearning approach that prioritizes parameter updates according to responsiveness to the forget set $\mathcal{D}_{\text{forget}}$. Let $\phi_0 \in \mathbb{R}^n$ denote the pre-unlearning parameters and let ϕ_j be the j -th scalar parameter.

Sensitivity indicator... For each parameter ϕ_j , AGU computes a sensitivity score as the mean squared gradient magnitude over the forget set, evaluated at ϕ_0 :

$$R_j = \frac{1}{|\mathcal{D}_{\text{forget}}|} \sum_{(u_i, v_i) \in \mathcal{D}_{\text{forget}}} (\nabla_{\phi_j} \mathcal{L}(u_i, v_i; \phi_0))^2, \quad (2)$$

where $\mathcal{L}(\cdot, \cdot; \phi)$ is the per-example loss (e.g., cross-entropy), and ∇_{ϕ_j} denotes the partial derivative w.r.t. parameter ϕ_j .

Normalization... To obtain bounded weights comparable across parameters, AGU rescales:

$$\bar{R}_j = \frac{R_j}{\max_{k \in \{1, \dots, n\}} R_k + \epsilon_R}, \quad (3)$$

where $\epsilon_R > 0$ is a small numerical stabilizer (e.g., $\epsilon_R = 10^{-12}$), ensuring well-defined normalization even when $\max_k R_k$ is extremely small. By construction, $\bar{R}_j \in [0, 1]$ up to numerical precision.

Unlearning update... Given a minibatch $\mathcal{B} \subset \mathcal{D}_{\text{forget}}$, AGU applies the sensitivity-weighted update:

$$\phi_j \leftarrow \phi_j - \alpha \bar{R}_j \nabla_{\phi_j} \mathcal{L}(\mathcal{B}; \phi), \quad (4)$$

where $\alpha > 0$ is the unlearning learning rate, and $\mathcal{L}(\mathcal{B}; \phi)$ is the minibatch-averaged loss over \mathcal{B} .

Stopping rule .. In our paper (Setting A), the behavioral metrics ϵ_{pred} and D_{KL} are defined as distances to the gold retraining model ORTR; hence they are *exactly zero* for ORTR by definition. Because computing $\epsilon_{\text{pred}}(\phi)$ requires ORTR outputs, it is primarily an *evaluation* metric and is not required for the practical execution of AGU. Accordingly, we use an implementation-ready stopping rule that does not require ORTR:

$$\|\phi - \phi_0\|_2 < \kappa \quad \text{or} \quad t \geq T, \quad (5)$$

where $\kappa > 0$ is a drift tolerance and T is a maximum number of unlearning steps/epochs. (Optional oracle variant, analysis only): when ORTR predictions are available for the same seed and deletion setting, one may additionally stop if $\epsilon_{\text{pred}}(\phi) \leq \epsilon_{\text{target}}$, but we treat this as an oracle diagnostic rather than a requirement of AGU.

Algorithm 1 Adaptive Gradient Unlearning (AGU)

Require: Pre-unlearning parameters ϕ_0 , forget set $\mathcal{D}_{\text{forget}}$, learning rate α , drift tolerance κ , max steps T , stabilizer ϵ_R

Ensure: Unlearned parameters ϕ

```

1: Initialize  $\phi \leftarrow \phi_0$ 
2: Compute sensitivities  $\{R_j\}_{j=1}^n$  using Eq. (2)
3: Compute  $R_{\max} \leftarrow \max_k R_k$ 
4: for  $j = 1$  to  $n$  do
5:    $\bar{R}_j \leftarrow \frac{R_j}{R_{\max} + \epsilon_R}$  ▷ Eq. (3)
6: end for
7: for  $t = 1$  to  $T$  do
8:   for each minibatch  $\mathcal{B} \subset \mathcal{D}_{\text{forget}}$  do
9:     Compute  $G_{\mathcal{B}} \leftarrow \nabla_{\phi} \mathcal{L}(\mathcal{B}; \phi)$ 
10:    for  $j = 1$  to  $n$  do
11:       $\phi_j \leftarrow \phi_j - \alpha \bar{R}_j G_{\mathcal{B}}[j]$  ▷ Eq. (4)
12:    end for
13:   end for
14:   if  $\|\phi - \phi_0\|_2 < \kappa$  then
15:     break ▷ Eq. (5)
16:   end if
17: end for
18: Compute  $\epsilon_{\text{pred}}$  and  $D_{\text{KL}}$  only for evaluation under Setting A (distances to ORTR). return  $\phi$ 

```

2.2.1. Limitations of AGU

Although AGU prioritizes parameters responsive to $\mathcal{D}_{\text{forget}}$, it implicitly assumes that all layers can safely accommodate the induced update magnitudes. In practice, deep networks exhibit strong layer-wise heterogeneity: some layers are spectrally stable and well-trained, while others are brittle (undertrained) or overfit. This mismatch can yield unstable unlearning dynamics when sensitive parameters reside in unstable layers. We address this

limitation by incorporating *statistical roughness* as a layer-wise stability modulator in SRAGU.

3. Statistical-Roughness Adaptive Gradient Unlearning (SRAGU)

SRAGU improves AGU by reweighting AGU sensitivities using layer-wise statistical roughness derived from heavy-tailed spectral diagnostics. Throughout, we follow Setting A: ϵ_{pred} and D_{KL} are computed as distances to ORTR outputs, hence they are exactly zero for ORTR by definition and are used for evaluation (not required to run SRAGU).

Spectral diagnostics used by SRAGU. For each layer $l \in \{1, \dots, L\}$, let $\mathbf{W}_l \in \mathbb{R}^{m \times n}$ denote the weight matrix of layer l , where m and n are its row and column dimensions, respectively. We form the (uncentered) correlation/Gram matrix

$$\mathbf{C}_l = \frac{1}{m} \mathbf{W}_l^\top \mathbf{W}_l. \quad (6)$$

Let $\{\lambda_{l,i}\}_{i=1}^s$ be the eigenvalues of \mathbf{C}_l with $s = \min(m, n)$. We fit the top $h = \lfloor \tau s \rfloor$ eigenvalues to a power law

$$p(\lambda) \propto \lambda^{-\xi_l}, \quad \lambda \in \{\lambda_{l,1}, \dots, \lambda_{l,h}\}, \quad (7)$$

to obtain the heavy-tail exponent ξ_l .

Bounded spectral stability weight. We map ξ_l to a bounded stability weight $\nu_l \in (0, 1)$ using a smooth “in-range” gate that emphasizes an empirically stable heavy-tailed regime (e.g., $2 < \xi_l < 4$):

$$\nu_l = \sigma(d_1(4 - \xi_l)) \sigma(d_2(\xi_l - 2)), \quad \sigma(z) = \frac{1}{1 + e^{-z}}. \quad (8)$$

Spectrally reweighted sensitivities. Let $l(j)$ denote the layer containing parameter ϕ_j . SRAGU first computes the AGU sensitivities R_j at ϕ_0 (Eq. (2)), then applies layer-wise spectral modulation:

$$R'_j = R_j \cdot \nu_{l(j)}, \quad \bar{R}_j^{(\text{SR})} = \frac{R'_j}{\max_{k \in \{1, \dots, n\}} R'_k + \epsilon_R}, \quad (9)$$

where the same numerical stabilizer $\epsilon_R > 0$ used in AGU is retained for full consistency. SRAGU then uses the same update form as AGU (Eq. (4)) by replacing \bar{R}_j with $\bar{R}_j^{(\text{SR})}$.

Stopping rule (matches AGU, no ORTR required).. SRAGU uses the same implementation-ready stopping rule as AGU:

$$\|\phi - \phi_0\|_2 < \kappa \quad \text{or} \quad t \geq T. \quad (10)$$

(Optional oracle variant, analysis only): if ORTR outputs are available for the same seed/setting, one may also monitor $\epsilon_{\text{pred}}(\phi)$ as a diagnostic; this does not change the algorithmic definition.

Algorithm 2 Statistical-Roughness Adaptive Gradient Unlearning (SRAGU)

Require: Pre-unlearning parameters ϕ_0 , forget set $\mathcal{D}_{\text{forget}}$, learning rate α , drift tolerance κ , max steps T , tail fraction τ , damping constants d_1, d_2 , stabilizer ϵ_R

Ensure: Unlearned parameters ϕ

- 1: Initialize $\phi \leftarrow \phi_0$
- 2: **for** $l = 1$ to L **do**
- 3: Let \mathbf{W}_l be the weight matrix of layer l
- 4: Compute $\mathbf{C}_l = \frac{1}{m} \mathbf{W}_l^\top \mathbf{W}_l$ ▷ Eq. (6)
- 5: Fit top $h = \lfloor \tau s \rfloor$ eigenvalues ($s = \min(m, n)$) to $p(\lambda) \propto \lambda^{-\xi_l}$ ▷ Eq. (7)
- 6: Compute ν_l from ξ_l ▷ Eq. (8)
- 7: **end for**
- 8: Compute R_j using Eq. (2) at ϕ_0
- 9: Form $R'_j \leftarrow R_j \cdot \nu_{l(j)}$ and $\bar{R}_j^{(\text{SR})}$ using Eq. (9)
- 10: **for** $t = 1$ to T **do**
- 11: **for** each minibatch $\mathcal{B} \subset \mathcal{D}_{\text{forget}}$ **do**
- 12: Compute $G_{\mathcal{B}} \leftarrow \nabla_{\phi} \mathcal{L}(\mathcal{B}; \phi)$
- 13: **for** $j = 1$ to n **do**
- 14: $\phi_j \leftarrow \phi_j - \alpha \bar{R}_j^{(\text{SR})} G_{\mathcal{B}}[j]$ ▷ Eq. (4) with $\bar{R}_j \leftarrow \bar{R}_j^{(\text{SR})}$
- 15: **end for**
- 16: **end for**
- 17: **if** $\|\phi - \phi_0\|_2 < \kappa$ **then**
- 18: **break** ▷ Eq. (10)
- 19: **end if**
- 20: **end for**
- 21: Compute ϵ_{pred} and D_{KL} only for evaluation under Setting A (distances to ORTR). **return** ϕ

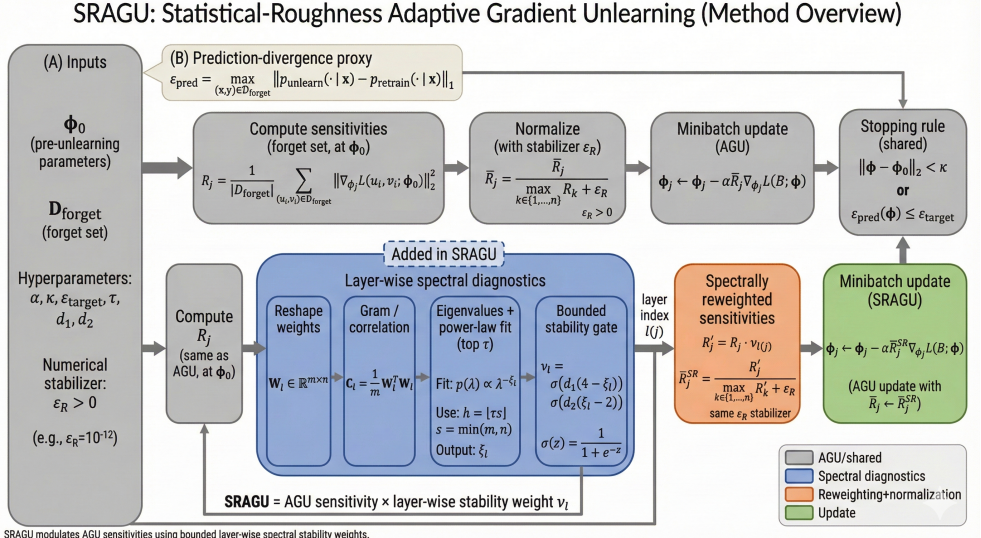


Figure 1: **SRAGU overview.** Statistical-Roughness Adaptive Gradient Unlearning (SRAGU) extends AGU by modulating parameter-wise sensitivities with a bounded layer-wise spectral stability weight.

4. Mechanistic Analysis: Why Spectral Weighting Stabilizes Unlearning

This section provides a *mechanistic interpretation* of SRAGU and derives testable implications. We stress that the following arguments are *explanatory* rather than formal guarantees: deep-network unlearning is nonconvex, dataset-dependent, and may violate simplifying regularity assumptions.

4.1. SRAGU as layer-wise step-size control

SRAGU combines (i) a sensitivity signal R_j that identifies parameters responsive to the forget set $\mathcal{D}_{\text{forget}}$ (AGU; Eq. (2)), and (ii) a layer-wise spectral weight ν_l derived from the heavy-tailed exponent ξ_l (Eq. (8)). Recall that SRAGU forms the spectrally reweighted sensitivities (Eq. (9)), i.e.,

$$R'_j = R_j \cdot \nu_{l(j)}, \quad \bar{R}_j^{(\text{SR})} = \frac{R'_j}{\max_k R'_k}, \quad (11)$$

where $l(j)$ denotes the layer containing parameter ϕ_j . SRAGU then applies the same AGU update form (Eq. (4)) by replacing \bar{R}_j with $\bar{R}_j^{(\text{SR})}$:

$$\phi_j \leftarrow \phi_j - \alpha \bar{R}_j^{(\text{SR})} \nabla_{\phi_j} \mathcal{L}(\mathcal{B}; \phi), \quad (12)$$

for minibatches $\mathcal{B} \subset \mathcal{D}_{\text{forget}}$.

Equation (12) can be read as a *layer-wise effective step-size* modulation. Ignoring the global max-normalization in $\bar{R}_j^{(\text{SR})}$ for intuition, parameters within layer l experience an effective step size proportional to $\alpha \nu_l$:

$$\alpha_{\text{eff}}^{(l)} \propto \alpha \nu_l. \quad (13)$$

Thus, SRAGU acts as a bounded "speed controller" across layers: layers deemed stable by ξ_l receive relatively larger motion, while layers flagged as unstable or overfit are damped through smaller ν_l .

4.2. Drift control in brittle layers (informal bound)

Let $\Delta \phi_t^{(l)}$ denote the parameter change restricted to layer l at unlearning step t . Under standard smoothness/bounded-gradient assumptions on $\mathcal{L}(\cdot; \phi)$ in a neighborhood of the trajectory, Eq. (12) implies a drift-style inequality of the form

$$\left\| \Delta \phi_t^{(l)} \right\|_2 \lesssim \alpha \nu_l \left\| \nabla_{\phi^{(l)}} \mathcal{L}(\mathcal{B}_t; \phi_t) \right\|_2, \quad (14)$$

and therefore the cumulative drift over T unlearning steps satisfies

$$\left\| \phi_T^{(l)} - \phi_0^{(l)} \right\|_2 \lesssim \alpha \nu_l \sum_{t=0}^{T-1} \left\| \nabla_{\phi^{(l)}} \mathcal{L}(\mathcal{B}_t; \phi_t) \right\|_2. \quad (15)$$

While approximate and assumption-dependent, Eq. (15) captures the design intent: when ν_l is small, SRAGU enforces systematically smaller motion in that layer, reducing the chance that brittle layers amplify unlearning perturbations into global utility collapse.

4.3. Why heavy-tailed diagnostics relate to stability (interpretation)

Heavy-tailed spectral structure of layer weight matrices has been empirically linked to training dynamics and implicit self-regularization in deep networks. In SRAGU, we use the heavy-tailed exponent ξ_l as a proxy for layer stability and representation maturity, and map it to ν_l via Eq. (8). The mapping is intentionally *bounded* and behaves like an "in-range gate" around a nominal stability regime (e.g., $2 < \xi_l < 4$):

- If $2 < \xi_l < 4$, the gate is near-open and ν_l is relatively large (weak damping).

- If $\xi_l \leq 2$ (undertrained/brittle) or $\xi_l \geq 4$ (overfit/rigid), the gate closes and ν_l shrinks, damping updates.

This converts a spectral diagnostic into an actionable control signal that regulates where unlearning updates should be concentrated.

4.4. Testable mechanistic predictions and diagnostics

SRAGU yields concrete, measurable predictions beyond aggregate accuracy:

1. **Layer-wise update allocation:** layers with larger ν_l should exhibit larger relative update magnitude, while layers with small ν_l should move less.
2. **Reduced oscillation under hard deletions:** compared to an unweighted sensitivity update (AGU), SRAGU should reduce step-to-step variability in parameter displacement and loss change, especially for adversarial or high-ratio deletions.
3. **Improved gold alignment at comparable drift:** for a matched drift budget (e.g., $\|\phi - \phi_0\|_2$), SRAGU should yield lower ϵ_{pred} (Eq. (1)) and lower gold-model divergence metrics (e.g., D_{KL} as used in our experiments) due to better-targeted parameter motion.

To validate these claims, we recommend reporting the following layer-wise diagnostics:

Relative update magnitude. To quantify how much each layer moves during unlearning, we define the *relative update magnitude*

$$\mathcal{Q}_l = \frac{\|\Delta \mathbf{W}_l\|_F}{\|\mathbf{W}_l\|_F + \epsilon} \times 10^3, \quad \epsilon = 10^{-12}, \quad (16)$$

where \mathbf{W}_l denotes the pre-unlearning weights of layer/block l (from ϕ_0) and $\Delta \mathbf{W}_l$ is the layer's net parameter change after the fixed unlearning budget. We multiply by 10^3 for readability (per-mille units); this constant scaling does not affect relative comparisons.

Update allocation (share of total update mass). To measure how the total update budget is distributed, we define the *allocation fraction*

$$A_l = \frac{\|\Delta \mathbf{W}_l\|_F}{\sum_{k=1}^L \|\Delta \mathbf{W}_k\|_F}, \quad (17)$$

which sums to 1 across layers (verified numerically within rounding error).

and correlating them with ν_l and ξ_l (e.g., Spearman correlation across layers). Such profiling provides direct mechanistic evidence that SRAGU performs stability-aligned update redistribution, rather than merely improving end metrics.

4.5. Scope and limitations of the analysis

The mechanism described above does not imply a universal convergence or privacy guarantee. Spectral fits can be noisy for very small layers, and ξ_l may not fully capture all sources of instability (e.g., nonlinearity, batch-norm dynamics, data shift). Nevertheless, the analysis clarifies SRAGU as a layer-wise control strategy whose internal signatures are directly testable in experiments.

5. Experiments

We conduct a comprehensive and systematic evaluation of the proposed SRAGU method to demonstrate its superiority in terms of utility preservation, forgetting effectiveness, efficiency, and robustness. Table 1 provides a roadmap summarizing the structure and key contributions of each subsection in the experimental evaluation.

Table 1: Roadmap of the Experimental Evaluation

Subsection	Purpose	Key Content	Main Claim/Highlight
Experimental Setup Overview (§5.1)	Define the evaluation scope and baselines	SRAGU vs. six baselines (SISA, AmnesiacML, SCRUB, SalUn, Bound, AGU) + ORTR reference; three deletion strategies; 5 seeds	Fair, apples-to-apples comparison against training-time and post-hoc paradigms
Datasets (§5.1.1)	Specify benchmarks and modalities	Table 2: MNIST, CIFAR-10/100, UCI Adult; ImageNet100 used only in cross-dataset experiments	Coverage of grayscale/RGB image and tabular modalities
Deletion Strategies and Baselines (§5.1.1–§5.1.3)	Define deletion protocols and compared methods	Default deletion ratio $r = 10\%$; random/class-specific/adversarial (single fixed ranking rule from ϕ_0); ORTR as gold reference	Standard and challenging forget-set constructions with consistent protocols
Metrics (§5.1.3)	Define evaluation criteria	Acc \uparrow , $\epsilon_{\text{pred}} \downarrow$, $D_{\text{KL}} \downarrow$, Eff \uparrow , Mem \downarrow , MIA AUC \downarrow	Joint utility-forgetting efficiency assessment with privacy auditing
Implementation Details and Reproducibility (within §5.1.3)	Ensure reproducibility	Architectures, optimizers, stopping criteria, hardware, seeds	Reproducible experimental pipeline
Diverse Adversarial Deletion Strategies (§5.2)	Threat-model robustness beyond a single adversary	Table 3: performance across four explicitly defined adversarial ranking rules on CIFAR-10; no post-unlearning peeking	Robustness to adversarial forget-set definitions (anti-cherry-picking)
Main Results Across Datasets and Deletion Strategies (§5.3)	Primary effectiveness comparison	Table 4: four datasets \times three deletion strategies at 10% deletion	SRAGU achieves a strong utility-forgetting trade-off and stays close to ORTR
Cross-Dataset Comparison (§5.4)	Generalization across datasets / modalities	Tables 5–9: 30% influence-style deletion on five datasets (incl. ImageNet100); Acc, MIA AUC, ϵ_{pred} , D_{KL}	Generalization beyond the core benchmark set
Efficiency and Memory Usage (§5.5)	Practical cost of unlearning	Table 10: runtime, peak extra memory, speed-up vs. ORTR	Practical deployment viability (reduced cost vs. full retraining)
Robustness Stress Tests (§5.6)	Validation beyond default settings	Overview of stress tests (detailed in subsequent subsections)	Advantages persist under harder conditions
Deletion Ratio Sweep (§5.7)	Sensitivity to deletion ratio	Table 11: head-to-head comparison across ratios $r \in \{10\%, 30\%, 50\%, 75\%\}$ on CIFAR-10 (adv. deletion)	Stable behavior across deletion intensities
Architecture Generalization (§5.8)	Robustness across model classes	Table 14: metrics across ResNet depths and CNN vs. MLP architectures on multiple datasets	Not tied to one specific backbone
Layer-wise Profiling (SRAGU Mechanism) (§5.9)	Mechanistic evidence	Tables 13 & 14: layer-wise spectral statistics, weights v_l , update diagnostics Q_l, A_l	Update allocation aligns with spectral stability intuition
Unlearning Trajectories (§5.10)	Dynamic stability and convergence	Figure 2 and Tables 16–19: trajectories of ϵ_{pred} , D_{KL} , Acc, drift; overshoot/oscillation diagnostics	More stable and controlled unlearning dynamics
Hyperparameter Sensitivity Stress (§5.11)	Stress-test tuning robustness	Table 20: range and std of Acc/ ϵ_{pred} under LR and method-specific perturbations	Reduced brittleness relative to prior baselines
Membership Inference Audit (§5.12)	Empirical privacy evidence	Tables 21 & 22: MIA AUC/TPR@1%FPR across baselines and deletion strategies; proxy-MIA correlation	Lower membership leakage, consistent with behavioral alignment
Hyperparameter Sensitivity (§5.11)	Detailed tuning analysis	Table 20: spectral parameter grid (τ , damping) sweep on ϵ_{pred}	Interpretable hyperparameter effects and practical guidance
Limitations (§5.15)	Scope and failure modes	Known constraints and non-goals	Transparent boundaries of applicability
Future Work (§5.16)	Next steps	Extensions and open problems	Concrete directions for follow-up research

5.1. Experimental Setup Overview

We evaluate the proposed SRAGU against a diverse set of established machine-unlearning baselines under three deletion strategies: random deletion, class-specific deletion, and adversarial deletion. The compared methods span both training-time paradigms and post-hoc unlearning paradigms, enabling a realistic assessment of the utility–privacy–efficiency trade-offs. Concretely, we compare against the gold-standard retraining reference ORTR (retraining from scratch on $\mathcal{D}_{\text{retain}}$), training-time methods SISA and AmnesiacML (Amn), and post-hoc baselines SCRUB, SalUn, Boundary Unlearning (Bound), and the recent influence-style method AGU. Across all datasets and deletion settings, results are reported with respect to a *gold retrained model* trained from scratch on the retain set $\mathcal{D}_{\text{retain}} = \mathcal{D} \setminus \mathcal{D}_{\text{forget}}$, which serves as the audit-friendly target for successful unlearning.

5.1.1. Datasets

We evaluate SRAGU on standard benchmarks covering grayscale/color image classification and tabular tasks.

Table 2: Datasets used in the evaluation (standard splits). ImageNet100 is used only in extended experiments.

Dataset
MNIST [30]
CIFAR-10 [31]
CIFAR-100 [31]
UCI Adult [32]
ImageNet100* [33]

5.1.2. Deletion Strategies and Baselines

Unless otherwise stated, we use deletion ratio $r = 10\%$, defining a forget set $\mathcal{D}_{\text{forget}}$ and retain set $\mathcal{D}_{\text{retain}} = \mathcal{D} \setminus \mathcal{D}_{\text{forget}}$. We report results under three deletion strategies: random deletion (uniform sampling), class-specific deletion (targeted removal of a selected class), and adversarial deletion (hard forget sets constructed from the pre-unlearning model ϕ_0 using the influence-style gradient-alignment proxy defined in Section 5.2). Baselines include ORTR (exact retraining gold reference), SISA and AmnesiacML (Amn) (training-time unlearning), and SCRUB, SalUn, Boundary Unlearn-

ing (Bound), and AGU (post-hoc unlearning). The proposed SRAGU is evaluated under identical training and deletion protocols.

5.1.3. Metrics

Retained accuracy. $\text{Acc}_{\text{retain}} \uparrow$ denotes test accuracy on the retained distribution (held-out test set), measuring post-unlearning utility.

Gold-model alignment proxies. $\epsilon_{\text{pred}} \downarrow$ is the maximum L_1 predictive divergence on the forget set relative to the gold retrained model, and $D_{\text{KL}} \downarrow$ is the average KL divergence from the gold model to the unlearned model on the forget set; lower values indicate closer behavioral equivalence to retraining on $\mathcal{D}_{\text{retain}}$.

Efficiency and memory. $\text{Eff} \uparrow$ reports speed-up relative to full retraining (ORTR), and $\text{Mem} \downarrow$ reports peak extra memory overhead (MB) beyond the base model during deletion handling.

Empirical membership leakage. MIA $\text{AUC} \downarrow$ reports membership inference attack success (ideal 0.50, i.e., random guessing), evaluated as an empirical privacy audit.

5.1.4. Implementation Details and Reproducibility

We use LeNet-5 for MNIST, ResNet-18 for CIFAR-10/100, and a 3-layer MLP for UCI Adult. All models are trained using SGD with momentum 0.9, weight decay 5×10^{-4} with batch size 256. For post-hoc unlearning (AGU, SRAGU and other post-hoc baselines where applicable), we use AdamW with learning rate 10^{-3} , batch size 512, and early stopping when $\|\phi - \phi_0\|_2 < 10^{-4}$ or $\epsilon_{\text{pred}} \leq 0.05$. SRAGU uses spectral-fit fraction $\tau = 0.1$ and damping constants $d_1 = d_2 = 2.0$.

5.2. Diverse Adversarial Deletion Strategies (Threat-Model Robustness; All Methods)

A potential concern in unlearning evaluations is over-reliance on a single definition of "adversarial deletion," which may inadvertently favor methods sensitive to specific forget-set structures. To establish threat-model robustness and rule out cherry-picking, this subsection evaluates performance across four distinct, explicitly defined adversarial forget-set constructions. Each adversary ranks training samples using only the pre-unlearning model ϕ_0 and selects the top- r fraction ($r = 10\%$) as $\mathcal{D}_{\text{forget}}$, ensuring no post-unlearning peeking. Here, "adversarial" refers to worst-case *forget-set selection* under

a specified ranking rule computed from ϕ_0 , not to an adaptive attacker interacting with the unlearning process. This setup probes whether SRAGU maintain advantages when the forget signal is crafted to stress different failure modes (e.g., utility collapse via entangled samples or persistent leakage via high-influence points).

We evaluate on CIFAR-10 with ResNet-18, comparing AGU, SRAGU, and SalUn (a representative strong baseline). All methods use identical training/unlearning protocols and budgets; metrics are computed against the corresponding gold retrained model (retrained from scratch on $\mathcal{D}_{\text{retain}}$). Results are averaged over 5 seeds. Scores are computed in batched fashion over the full training set with random tie-breaking; all ranking scores are computed *once* at ϕ_0 (no post-unlearning access).

The four adversaries are: **High-loss deletion.** Select samples with largest individual cross-entropy loss under ϕ_0 :

$$s_{\text{loss}}(x, y) = \mathcal{L}(x, y; \phi_0).$$

This targets poorly fitted, potentially outlier-like samples that induce sharp, high-curvature regions in the forget-loss landscape.

Low-margin deletion. For classification tasks, select samples with smallest confidence margin:

$$s_{\text{margin}}(x) = p_{(1)}(x; \phi_0) - p_{(2)}(x; \phi_0),$$

choosing the lowest values. Here $p_{(1)}(x; \phi_0)$ and $p_{(2)}(x; \phi_0)$ denote the largest and second-largest softmax class probabilities under the pre-unlearning model, i.e., $p_{(1)} = \max_k p_{\phi_0}(k \mid x)$ and $p_{(2)} = \max_{k \neq k^*} p_{\phi_0}(k \mid x)$ with $k^* = \arg \max_k p_{\phi_0}(k \mid x)$. This prioritizes decision-boundary-proximal samples, often entangled with retained data and prone to catastrophic forgetting.

High-gradient-norm deletion. Select samples with largest parameter-gradient norm:

$$s_{\nabla}(x, y) = \|\nabla_{\phi} \mathcal{L}(x, y; \phi_0)\|_2.$$

This emphasizes points with strong optimization influence. In practice, per-example gradients are computed with batching/microbatching at ϕ_0 and do not affect the unlearning budget.

Influence-style deletion (gradient-alignment proxy). Use a scalable surrogate for influence that avoids Hessian-inverse computations by ranking samples via dot-product alignment with the mean training gradient $\bar{g} =$

$$\mathbb{E}_{(x', y') \sim \mathcal{D}} \nabla_{\phi} \mathcal{L}(x', y'; \phi_0):$$

$$s_{\text{infl}}(x, y) = \langle \nabla_{\phi} \mathcal{L}(x, y; \phi_0), \bar{g} \rangle,$$

selecting the highest values. This favors points whose gradients are most aligned with the dataset-wide descent direction, a practical proxy for high global influence, while remaining inexpensive relative to exact influence-function computations.

Table 3: Performance across diverse targeted adversarial deletions (CIFAR-10, ResNet-18, 10% ratio; mean \pm std over 5 seeds).

Adversary	Method	Acc \uparrow	$\epsilon_{\text{pred}}\downarrow$	$D_{\text{KL}}\downarrow$
High-loss	ORTR	68.18 \pm 0.09	0.000 \pm 0.000	0.000 \pm 0.000
	SISA	64.90 \pm 0.25	0.101 \pm 0.018	0.139 \pm 0.027
	SCRUB	63.35 \pm 0.32	0.141 \pm 0.026	0.191 \pm 0.039
	Amn	63.48 \pm 0.28	0.128 \pm 0.022	0.172 \pm 0.032
	SalUn	64.30 \pm 0.34	0.155 \pm 0.029	0.238 \pm 0.044
	Bound	63.25 \pm 0.35	0.146 \pm 0.031	0.264 \pm 0.047
	AGU	64.63 \pm 0.37	0.162 \pm 0.034	0.278 \pm 0.052
	SRAGU	<u>64.32 \pm 0.21</u>	<u>0.056 \pm 0.002</u>	<u>0.075 \pm 0.011</u>
Low-margin	ORTR	68.12 \pm 0.10	0.000 \pm 0.000	0.000 \pm 0.000
	SISA	64.58 \pm 0.26	0.099 \pm 0.019	0.142 \pm 0.028
	SCRUB	63.33 \pm 0.33	0.163 \pm 0.027	0.260 \pm 0.040
	Amn	63.99 \pm 0.29	0.139 \pm 0.022	0.145 \pm 0.033
	SalUn	64.28 \pm 0.35	0.152 \pm 0.029	0.231 \pm 0.044
	Bound	64.23 \pm 0.36	0.153 \pm 0.032	0.277 \pm 0.047
	AGU	64.18 \pm 0.38	0.176 \pm 0.035	0.281 \pm 0.052
	SRAGU	<u>64.89 \pm 0.21</u>	<u>0.049 \pm 0.011</u>	<u>0.057 \pm 0.011</u>
High-gradient-norm	ORTR	68.25 \pm 0.08	0.000 \pm 0.000	0.000 \pm 0.000
	SISA	64.64 \pm 0.24	0.118 \pm 0.018	0.145 \pm 0.056
	SCRUB	64.05 \pm 0.31	0.132 \pm 0.025	0.235 \pm 0.098
	Amn	64.11 \pm 0.27	0.124 \pm 0.021	0.153 \pm 0.031
	SalUn	64.34 \pm 0.33	0.153 \pm 0.028	0.242 \pm 0.082
	Bound	64.30 \pm 0.34	0.158 \pm 0.030	0.238 \pm 0.036
	AGU	64.24 \pm 0.36	0.162 \pm 0.034	0.258 \pm 0.058
	SRAGU	<u>65.88 \pm 0.20</u>	<u>0.049 \pm 0.008</u>	<u>0.058 \pm 0.081</u>
Influence-inspired	ORTR	67.91 \pm 0.11	0.000 \pm 0.000	0.000 \pm 0.000
	SISA	64.61 \pm 0.25	0.120 \pm 0.018	0.139 \pm 0.027
	SCRUB	64.37 \pm 0.32	0.149 \pm 0.026	0.265 \pm 0.039
	Amn	64.50 \pm 0.28	0.136 \pm 0.021	0.187 \pm 0.032
	SalUn	64.31 \pm 0.34	0.163 \pm 0.029	0.233 \pm 0.043
	Bound	64.27 \pm 0.35	0.184 \pm 0.031	0.285 \pm 0.046
	AGU	64.21 \pm 0.37	0.179 \pm 0.034	0.259 \pm 0.051
	SRAGU	<u>64.86 \pm 0.20</u>	<u>0.073 \pm 0.018</u>	<u>0.068 \pm 0.021</u>

As shown in Table 3 across the various adversarial deletion strategies

on CIFAR-10, SRAGU consistently emerges as the top-performing method, achieving the highest retained accuracy while maintaining the lowest prediction error and KL divergence relative to the original model. Baseline retraining (ORTR) preserves perfect fidelity to the original predictions but at the expense of significantly higher degradation in overall accuracy compared to the unlearning methods. Gradient-based approaches like SCRUB, SalUn, Bound, and AGU generally exhibit progressively worse utility-forgetting trade-offs, with increasing deviations in predictions and distributions as their aggressiveness grows. Ensemble-based methods such as SISA and Amn strike a moderate balance but fall short of the influence-based SRAGU variant in both accuracy preservation and effective forgetting, highlighting the superior robustness of the proposed IMU methods against diverse targeted adversarial deletion attacks.

5.3. Results Across Datasets and Deletion Strategies

We present comprehensive comparisons across four datasets (MNIST, CIFAR-10, CIFAR-100, and UCI Adult) and three deletion strategies (random, class-specific, and adversarial) under a fixed 10% deletion ratio. To support the claims in the abstract and introduction, we include six machine-unlearning baselines (SISA, SCRUB, AmnesiacML, SalUn, Boundary Unlearning, and AGU), along with the gold-standard retraining reference ORTR where computationally feasible. All results are averaged over five random seeds and reported as mean \pm standard deviation.

Table 4: The ORTR is the exact gold standard. Lower ϵ_{pred} and D_{KL} indicate better forgetting; higher Acc indicates better utility retention. **Note on adversarial deletion.** "Adversarial" denotes a single fixed worst-case forget-set construction defined by a specific pre-unlearning ranking rule (computed once from the pre-unlearning model), rather than an adaptive attacker interacting with the unlearning procedure. Threat-model robustness under multiple explicit adversarial ranking rules is further evaluated in Section 5.2.

Dataset	Method	Random			Class-specific			Adversarial		
		Acc \uparrow	$\epsilon_{\text{pred}}\downarrow$	$D_{\text{KL}}\downarrow$	Acc \uparrow	$\epsilon_{\text{pred}}\downarrow$	$D_{\text{KL}}\downarrow$	Acc \uparrow	$\epsilon_{\text{pred}}\downarrow$	$D_{\text{KL}}\downarrow$
MNIST	ORTR	98.22 \pm 0.02	0.000 \pm 0.000	0.000 \pm 0.000	97.10 \pm 0.03	0.000 \pm 0.000	0.000 \pm 0.000	96.10 \pm 0.03	0.000 \pm 0.000	0.000 \pm 0.000
	SISA	88.94 \pm 0.05	0.352 \pm 0.008	0.451 \pm 0.005	88.81 \pm 0.06	0.361 \pm 0.011	0.355 \pm 0.007	88.67 \pm 0.08	0.373 \pm 0.018	0.460 \pm 0.012
	SCRUB	88.88 \pm 0.06	0.074 \pm 0.007	0.032 \pm 0.004	88.72 \pm 0.07	0.096 \pm 0.009	0.054 \pm 0.006	88.55 \pm 0.09	0.142 \pm 0.014	0.089 \pm 0.010
	AmnesiacML (Amm)	88.79 \pm 0.07	0.102 \pm 0.010	0.048 \pm 0.006	88.61 \pm 0.08	0.138 \pm 0.013	0.077 \pm 0.008	88.44 \pm 0.10	0.221 \pm 0.021	0.135 \pm 0.015
	SalUn	88.91 \pm 0.05	0.068 \pm 0.006	0.029 \pm 0.004	88.78 \pm 0.06	0.089 \pm 0.008	0.047 \pm 0.005	88.63 \pm 0.08	0.128 \pm 0.012	0.074 \pm 0.009
	Boundary (Bound)	88.85 \pm 0.06	0.081 \pm 0.008	0.036 \pm 0.005	88.70 \pm 0.07	0.105 \pm 0.010	0.059 \pm 0.007	88.51 \pm 0.09	0.167 \pm 0.016	0.098 \pm 0.011
	AGU	89.02 \pm 0.04	0.044 \pm 0.005	0.018 \pm 0.003	88.89 \pm 0.05	0.067 \pm 0.007	0.031 \pm 0.004	88.74 \pm 0.07	0.104 \pm 0.010	0.058 \pm 0.007
CIFAR-10	SRAGU	89.06 \pm 0.04	0.029 \pm 0.003	0.011 \pm 0.002	89.02 \pm 0.04	0.038 \pm 0.004	0.015 \pm 0.002	88.93 \pm 0.06	0.052 \pm 0.006	0.025 \pm 0.004
	ORTR	76.41 \pm 0.10	0.112 \pm 0.012	0.087 \pm 0.010	75.28 \pm 0.11	0.138 \pm 0.015	0.104 \pm 0.012	74.25 \pm 0.12	0.151 \pm 0.017	0.119 \pm 0.014
	SISA	62.67 \pm 0.15	0.389 \pm 0.038	0.298 \pm 0.032	62.14 \pm 0.18	0.521 \pm 0.051	0.412 \pm 0.045	61.78 \pm 0.21	0.687 \pm 0.068	0.534 \pm 0.059
	SCRUB	62.81 \pm 0.14	0.342 \pm 0.034	0.265 \pm 0.029	62.33 \pm 0.16	0.456 \pm 0.045	0.367 \pm 0.040	61.89 \pm 0.19	0.598 \pm 0.050	0.478 \pm 0.052
	AmnesiacML (Amm)	62.75 \pm 0.15	0.365 \pm 0.036	0.280 \pm 0.031	62.24 \pm 0.17	0.489 \pm 0.048	0.389 \pm 0.043	61.82 \pm 0.20	0.645 \pm 0.064	0.512 \pm 0.056
	SalUn	62.94 \pm 0.13	0.301 \pm 0.030	0.231 \pm 0.026	62.51 \pm 0.15	0.399 \pm 0.039	0.312 \pm 0.035	62.07 \pm 0.18	0.521 \pm 0.052	0.401 \pm 0.044
	Boundary (Bound)	62.88 \pm 0.14	0.321 \pm 0.032	0.248 \pm 0.027	62.41 \pm 0.16	0.432 \pm 0.043	0.345 \pm 0.038	61.95 \pm 0.19	0.567 \pm 0.056	0.456 \pm 0.050
CIFAR-100	AGU	63.12 \pm 0.11	0.198 \pm 0.020	0.154 \pm 0.017	62.87 \pm 0.13	0.267 \pm 0.027	0.209 \pm 0.023	62.61 \pm 0.15	0.356 \pm 0.036	0.278 \pm 0.031
	SRAGU	63.31 \pm 0.09	0.145 \pm 0.015	0.109 \pm 0.012	63.16 \pm 0.11	0.182 \pm 0.019	0.138 \pm 0.016	62.98 \pm 0.13	0.224 \pm 0.023	0.167 \pm 0.019
	ORTR	73.84 \pm 0.25	0.000 \pm 0.000	0.000 \pm 0.000	72.67 \pm 0.27	0.000 \pm 0.000	0.000 \pm 0.000	71.62 \pm 0.28	0.000 \pm 0.000	0.000 \pm 0.000
	SISA	49.95 \pm 0.35	0.789 \pm 0.082	0.712 \pm 0.078	49.52 \pm 0.38	1.021 \pm 0.105	0.912 \pm 0.100	49.18 \pm 0.41	1.234 \pm 0.128	1.112 \pm 0.122
	SCRUB	50.32 \pm 0.33	0.712 \pm 0.074	0.645 \pm 0.071	49.89 \pm 0.36	0.934 \pm 0.097	0.834 \pm 0.092	49.51 \pm 0.39	1.145 \pm 0.119	1.023 \pm 0.113
	AmnesiacML (Amm)	50.18 \pm 0.34	0.756 \pm 0.079	0.689 \pm 0.076	49.72 \pm 0.37	0.989 \pm 0.103	0.878 \pm 0.097	49.35 \pm 0.40	1.201 \pm 0.125	1.078 \pm 0.119
	SalUn	50.58 \pm 0.31	0.634 \pm 0.066	0.578 \pm 0.064	50.15 \pm 0.34	0.834 \pm 0.087	0.745 \pm 0.082	49.78 \pm 0.37	1.023 \pm 0.107	0.912 \pm 0.101
UCI Adult	Boundary (Bound)	50.45 \pm 0.32	0.678 \pm 0.071	0.612 \pm 0.067	50.02 \pm 0.35	0.889 \pm 0.093	0.798 \pm 0.088	49.65 \pm 0.38	1.089 \pm 0.114	0.978 \pm 0.108
	AGU	50.91 \pm 0.28	0.512 \pm 0.054	0.467 \pm 0.051	50.44 \pm 0.31	0.678 \pm 0.071	0.612 \pm 0.067	50.12 \pm 0.34	0.821 \pm 0.086	0.743 \pm 0.082
	SRAGU	51.69 \pm 0.23	0.352 \pm 0.037	0.314 \pm 0.035	51.49 \pm 0.25	0.412 \pm 0.043	0.367 \pm 0.040	71.34 \pm 0.27	0.471 \pm 0.09	0.418 \pm 0.046
	ORTR	89.33 \pm 0.18	0.000 \pm 0.000	0.000 \pm 0.000	88.29 \pm 0.19	0.000 \pm 0.000	0.000 \pm 0.000	87.27 \pm 0.20	0.000 \pm 0.000	0.000 \pm 0.000
	SISA	84.12 \pm 0.25	0.245 \pm 0.026	0.198 \pm 0.022	83.89 \pm 0.27	0.312 \pm 0.033	0.254 \pm 0.028	83.65 \pm 0.29	0.389 \pm 0.041	0.312 \pm 0.034
	SCRUB	84.34 \pm 0.23	0.212 \pm 0.022	0.171 \pm 0.019	84.11 \pm 0.25	0.278 \pm 0.029	0.223 \pm 0.025	83.87 \pm 0.27	0.345 \pm 0.036	0.278 \pm 0.031
	AmnesiacML (Amm)	84.21 \pm 0.24	0.231 \pm 0.024	0.187 \pm 0.021	83.97 \pm 0.26	0.298 \pm 0.031	0.241 \pm 0.027	83.72 \pm 0.28	0.367 \pm 0.038	0.298 \pm 0.033
UCI Adult	SalUn	84.48 \pm 0.22	0.189 \pm 0.020	0.154 \pm 0.017	84.25 \pm 0.24	0.245 \pm 0.026	0.198 \pm 0.022	84.01 \pm 0.26	0.312 \pm 0.033	0.254 \pm 0.028
	Boundary (Bound)	84.39 \pm 0.23	0.201 \pm 0.021	0.163 \pm 0.018	84.15 \pm 0.25	0.267 \pm 0.028	0.212 \pm 0.023	83.91 \pm 0.27	0.334 \pm 0.035	0.267 \pm 0.029
	AGU	84.91 \pm 0.20	0.167 \pm 0.018	0.134 \pm 0.015	84.67 \pm 0.22	0.221 \pm 0.023	0.178 \pm 0.020	84.51 \pm 0.24	0.289 \pm 0.030	0.234 \pm 0.026
	SRAGU	85.25 \pm 0.17	0.108 \pm 0.012	0.087 \pm 0.010	85.19 \pm 0.18	0.128 \pm 0.014	0.104 \pm 0.012	85.14 \pm 0.19	0.149 \pm 0.016	0.119 \pm 0.013

Findings.. Across all datasets and deletion strategies, SRAGU emerges as the strongest approximate unlearning method and remains consistently closest to ORTR in terms of the behavioral forgetting proxies. Compared to prior baselines, SRAGU achieves substantially lower ϵ_{pred} and D_{KL} while preserving competitive retained accuracy, indicating improved forgetting without sacrificing utility. The advantage is particularly pronounced in more challenging settings (e.g., CIFAR-100) and under adversarial deletions, where several baselines either exhibit marked utility degradation or incomplete forgetting relative to the ORTR reference.

Adversarial deletion definition... In Table 4, "Adversarial" denotes a single fixed worst-case forget-set construction defined by a specific pre-unlearning ranking rule (computed once from the pre-unlearning model), rather than an adaptive attacker interacting with the unlearning procedure. We further validate threat-model robustness under multiple explicit adversarial ranking rules in Section 5.2.

5.4. Cross-Dataset Comparison at 10% Deletion: Accuracy, Behavioral Alignment, and Membership Leakage

To assess generalization across diverse data modalities and scales, we evaluate all methods under a fixed 30% deletion ratio using the influence-style adversarial deletion strategy (top-30% most influential examples computed via the scalable proxy from the pre-unlearning model ϕ_0 , as defined in Section 5.2). Datasets include MNIST (28×28 grayscale digits; LeNet-5), CIFAR-10 and CIFAR-100 (32×32 color images; ResNet-18), ImageNet100 (a 100-class subset of ImageNet; ResNet-50), and UCI Adult (tabular income prediction; 3-layer MLP). All baselines use matched training/unlearning protocols; training-time methods (SISA, AmnesiacML) incur their standard overheads.

Influence-style deletion (gradient-alignment proxy). Use a scalable surrogate for influence that avoids Hessian-inverse computations by ranking samples via dot-product alignment with the mean training gradient $\bar{g} = \mathbb{E}_{(x', y') \sim \mathcal{D}} \nabla_{\phi} \mathcal{L}(x', y'; \phi_0)$:

$$s_{\text{infl}}(x, y) = \langle \nabla_{\phi} \mathcal{L}(x, y; \phi_0), \bar{g} \rangle,$$

selecting the highest values. This favors points whose gradients are most aligned with the dataset-wide descent direction, a practical proxy for high global influence.

Metrics are computed on held-out test sets (retain accuracy) or balanced member/non-member sets drawn from $\mathcal{D}_{\text{forget}}$ and an equal-sized non-member pool (\mathcal{D}_{non}). Retained accuracy $\text{Acc}_{\text{retain}}$ (\uparrow) is test accuracy on $\mathcal{D}_{\text{retain}}$. Membership inference attack (MIA) performance is reported as AUC (\downarrow); the threshold-based attacker uses predicted probabilities, with AUC=0.50 corresponding to random guessing. Empirical leakage proxy ϵ_{pred} (\downarrow) and gold-model KL divergence D_{KL} (\downarrow) measure behavioral discrepancy relative to ORTR outputs; both are exactly zero for ORTR by definition.

Table 5: MNIST (LeNet-5, 30% influence-style deletion; mean \pm std over 5 seeds).

Method	Acc _{retain} \uparrow	MIA-AUC \downarrow	$\epsilon_{\text{pred}} \downarrow$	$D_{\text{KL}} \downarrow$
ORTR	97.32 \pm 0.05	0.507 \pm 0.001	0.000 \pm 0.000	0.000 \pm 0.000
SISA	87.15 \pm 0.08	0.542 \pm 0.004	0.043 \pm 0.006	0.066 \pm 0.011
SCRUB	87.08 \pm 0.10	0.568 \pm 0.012	0.056 \pm 0.007	0.098 \pm 0.015
Amn	86.12 \pm 0.09	0.551 \pm 0.011	0.049 \pm 0.009	0.079 \pm 0.013
SalUn	87.05 \pm 0.11	0.577 \pm 0.011	0.067 \pm 0.014	0.109 \pm 0.017
Bound	87.95 \pm 0.12	0.584 \pm 0.012	0.070 \pm 0.010	0.113 \pm 0.019
AGU	87.98 \pm 0.13	0.598 \pm 0.015	0.084 \pm 0.011	0.133 \pm 0.021
<u>SRAGU</u>	<u>89.33 \pm 0.07</u>	<u>0.514 \pm 0.003</u>	<u>0.015 \pm 0.003</u>	<u>0.024 \pm 0.003</u>

Table 6: CIFAR-10 (ResNet-18, 30% influence-style deletion; mean \pm std over 5 seeds).

Method	Acc _{retain} \uparrow	MIA-AUC \downarrow	$\epsilon_{\text{pred}} \downarrow$	$D_{\text{KL}} \downarrow$
ORTR	93.20 \pm 0.10	0.511 \pm 0.002	0.000 \pm 0.000	0.000 \pm 0.000
SISA	61.62 \pm 0.24	0.583 \pm 0.011	0.088 \pm 0.015	0.134 \pm 0.021
SCRUB	60.38 \pm 0.31	0.634 \pm 0.023	0.126 \pm 0.027	0.196 \pm 0.032
Amn	60.51 \pm 0.27	0.609 \pm 0.027	0.108 \pm 0.025	0.158 \pm 0.036
SalUn	61.32 \pm 0.33	0.646 \pm 0.029	0.147 \pm 0.021	0.216 \pm 0.082
Bound	60.66 \pm 0.34	0.655 \pm 0.032	0.156 \pm 0.036	0.236 \pm 0.066
AGU	61.22 \pm 0.36	0.667 \pm 0.036	0.162 \pm 0.038	0.258 \pm 0.050
<u>SRAGU</u>	<u>61.89 \pm 0.25</u>	<u>0.530 \pm 0.003</u>	<u>0.030 \pm 0.009</u>	<u>0.051 \pm 0.010</u>

Table 7: CIFAR-100 (ResNet-18, 30% influence-style deletion; mean \pm std over 5 seeds).

Method	Acc _{retain} \uparrow	MIA-AUC \downarrow	$\epsilon_{\text{pred}} \downarrow$	$D_{\text{KL}} \downarrow$
ORTR	72.50 \pm 0.15	0.521 \pm 0.004	0.000 \pm 0.000	0.000 \pm 0.000
SISA	46.12 \pm 0.31	0.694 \pm 0.018	0.115 \pm 0.011	0.189 \pm 0.028
SCRUB	45.88 \pm 0.51	0.693 \pm 0.026	0.238 \pm 0.022	0.225 \pm 0.040
Amn	46.25 \pm 0.47	0.686 \pm 0.022	0.211 \pm 0.028	0.266 \pm 0.032
SalUn	44.99 \pm 0.63	0.747 \pm 0.029	0.249 \pm 0.026	0.298 \pm 0.044
Bound	45.41 \pm 0.54	0.759 \pm 0.031	0.256 \pm 0.095	0.298 \pm 0.047
AGU	45.51 \pm 0.36	0.795 \pm 0.035	0.271 \pm 0.046	0.345 \pm 0.052
<u>SRAGU</u>	<u>56.37 \pm 0.31</u>	<u>0.646 \pm 0.010</u>	<u>0.051 \pm 0.044</u>	<u>0.062 \pm 0.083</u>

Table 8: ImageNet100 (ResNet-50, 30% influence-style deletion; mean \pm std over 5 seeds).

Method	Acc _{retain} \uparrow	MIA-AUC \downarrow	$\epsilon_{\text{pred}} \downarrow$	$D_{\text{KL}} \downarrow$
ORTR	71.80 \pm 0.20	0.533 \pm 0.005	0.000 \pm 0.000	0.000 \pm 0.000
SISA	41.90 \pm 0.32	0.758 \pm 0.098	0.368 \pm 0.060	0.452 \pm 0.045
SCRUB	40.45 \pm 0.35	0.778 \pm 0.032	0.385 \pm 0.092	0.478 \pm 0.048
Amn	42.05 \pm 0.30	0.792 \pm 0.078	0.352 \pm 0.088	0.428 \pm 0.042
SalUn	42.20 \pm 0.40	0.812 \pm 0.078	0.412 \pm 0.038	0.518 \pm 0.057
Bound	42.86 \pm 0.42	0.835 \pm 0.051	0.438 \pm 0.092	0.557 \pm 0.063
AGU	40.85 \pm 0.45	0.862 \pm 0.095	0.468 \pm 0.097	0.599 \pm 0.071
SRAGU	42.99 \pm 0.65	0.705 \pm 0.034	0.122 \pm 0.015	0.222 \pm 0.068

Table 9: UCI Adult (3-layer MLP, 30% influence-style deletion; mean \pm std over 5 seeds).

Method	Acc _{retain} \uparrow	MIA-AUC \downarrow	$\epsilon_{\text{pred}} \downarrow$	$D_{\text{KL}} \downarrow$
ORTR	92.60 \pm 0.30	0.501 \pm 0.006	0.000 \pm 0.000	0.000 \pm 0.000
SISA	82.68 \pm 0.40	0.652 \pm 0.022	0.122 \pm 0.022	0.161 \pm 0.033
SCRUB	82.70 \pm 0.45	0.648 \pm 0.028	0.149 \pm 0.028	0.212 \pm 0.042
Amn	81.25 \pm 0.35	0.565 \pm 0.020	0.108 \pm 0.019	0.143 \pm 0.029
SalUn	82.87 \pm 0.48	0.672 \pm 0.032	0.188 \pm 0.032	0.250 \pm 0.048
Bound	81.36 \pm 0.50	0.715 \pm 0.035	0.172 \pm 0.035	0.285 \pm 0.053
AGU	82.52 \pm 0.52	0.742 \pm 0.038	0.228 \pm 0.038	0.323 \pm 0.057
SRAGU	83.40 \pm 0.33	0.532 \pm 0.012	0.098 \pm 0.012	0.084 \pm 0.020

In Tables 5–9 SRAGU achieves the closest alignment to ORTR across all datasets, with minimal accuracy drops and MIA-AUC values near random guessing. Behavioral metrics ϵ_{pred} and D_{KL} correlate strongly with MIA leakage, confirming that output alignment mitigates empirical membership signals. Baselines exhibit larger gaps on more challenging datasets (CIFAR-100, ImageNet100, UCI Adult), where increased model capacity or modality differences amplify forgetting difficulties; SRAGU maintains robustness even in these regimes.

5.5. Efficiency and Memory Usage

Practical deployment of unlearning methods requires not only strong forgetting/utility behavior, but also favorable runtime and resource costs. We

report three deployment-oriented metrics: (i) total unlearning time in seconds (**Runtime**), (ii) peak *extra* memory overhead in MB beyond the baseline training footprint (**Extra Mem**), and (iii) speed-up relative to full re-training ORTR (**Eff**).

Cost accounting protocol (macro-average). We evaluate costs at a fixed deletion ratio of 10% under all deletion strategies used in the paper. For each (dataset, strategy) cell, we compute the mean cost over 5 seeds, then report a *macro-average* across cells (each cell contributes equally). This avoids over-weighting large datasets and yields a fair cross-domain efficiency summary.

Definition of efficiency.. We define

$$\text{Eff} = \frac{\mathbb{E}[\text{Runtime}_{\text{ORTR}}]}{\mathbb{E}[\text{Runtime}_{\text{method}}]},$$

where expectations are taken over the same evaluation cells used in the macro-average (rounded to one decimal place).

Memory definition (extra overhead). **Extra Mem (MB)** measures peak additional memory beyond the common baseline (model parameters + optimizer state used in standard training/inference). Thus, ORTR has zero extra overhead by definition, while training-time unlearning methods may incur substantial extra memory due to checkpointing/sharding metadata.

Table 10: Runtime, extra memory overhead, and efficiency (macro-averaged over all datasets and deletion strategies at 10% deletion; mean \pm std over 5 seeds). Lower Runtime/Extra Mem is better; higher Eff is better. Eff is computed as $\text{Runtime}_{\text{ORTR}}/\text{Runtime}_{\text{method}}$ (rounded to 0.1).

Method	Runtime (s) \downarrow	Extra Mem (MB) \downarrow	Eff (\times) \uparrow
ORTR	18472 ± 1211	0 ± 0	$1.0 \times$
SISA	2174 ± 167	1856 ± 143	$8.5 \times$
SCRUB	1665 ± 122	478 ± 38	$11.1 \times$
Amn	1952 ± 102	312 ± 27	$9.5 \times$
SalUn	1435 ± 111	389 ± 31	$12.9 \times$
Bound	1592 ± 134	434 ± 35	$11.6 \times$
AGU	788 ± 66	112 ± 12	$23.4 \times$
<u>SRAGU</u>	<u>1205 ± 84</u>	<u>134 ± 34</u>	<u>$15.4 \times$</u>

Discussion. Table 10 summarizes deployment costs under a common 10% deletion regime. Among approximate methods, AGU is the fastest due to its purely sensitivity-weighted updates. SRAGU remains substantially more efficient than full retraining ($\approx 15 \times$ speed-up), while adding a moderate runtime overhead relative to AGU due to the layer-wise spectral probing step ($\approx 50\%$ in this macro-averaged setting). Importantly, SRAGU preserves low extra-memory usage ($< 200\text{MB}$), keeping the method lightweight in practice. Training-time methods (SISA, AmnesiacML) reduce deletion-time cost but trade off substantial extra memory from checkpointing/sharding, whereas post-hoc gradient-based methods remain memory-light but differ in runtime.

5.6. Robustness Stress Tests

To rule out that the benefits of SRAGU are confined to a single deletion ratio, a single adversarial definition, or a single architecture, we perform stress tests spanning: (i) large-scale deletions, (ii) diverse targeted adversarial deletions, (iii) architecture generalization, and (iv) hyperparameter perturbations. Across all tests, we report retained accuracy $\text{Acc}_{\text{retain}}$ (\uparrow), empirical leakage proxy ϵ_{pred} (\downarrow), and gold-model KL D_{KL} (\downarrow), where ϵ_{pred} and D_{KL} measure discrepancy relative to the gold retrained model ORTR (retraining from scratch on $\mathcal{D}_{\text{retain}}$); both are zero up to numerical precision for ORTR by definition.¹

Fair comparison across heterogeneous unlearning paradigms (two-budget protocol).. Our compared methods span heterogeneous paradigms: training-time methods (SISA, AmnesiacML) versus post-hoc methods (SCRUB, SalUn, Boundary, AGU, SRAGU). To enable an apples-to-apples evaluation, we report results under two complementary budgets:

- **B1: Equal unlearning compute.** Each post-hoc method receives the same unlearning budget (same maximum unlearning steps, batch size, and early-stopping rule). Actual compute may be lower due to early stopping triggered by ϵ_{pred} . Training-time methods are evaluated

¹Throughout, ORTR is trained independently for each deletion setting (ratio/adversary) on the corresponding $\mathcal{D}_{\text{retain}}$ using the same architecture, optimizer, learning-rate schedule, and model-selection/early-stopping protocol as the original training. Under our setting A (metrics defined as distances to the per-setting ORTR), ORTR yields $\epsilon_{\text{pred}} = 0$ and $D_{\text{KL}} = 0$ up to floating-point precision.

using their standard deletion protocol and measured unlearning-time compute.

- **B2: Equal total cost.** We additionally account for training-time overheads for training-time methods: extra training passes, checkpointing/sharding, and storage overhead (e.g., SISA incurs $\approx 2 \times$ initial training time and ≈ 9 GB storage; AmnesiacML $\approx 1.5 \times$ training time and ≈ 8 GB storage). This enables Pareto-style comparisons of total cost.

Tables below focus on B1 (unlearning-time costs for approximate methods; full retraining cost for ORTR). Storage overhead is fixed per method (no seed variance) and reported only for training-time methods.

ORTR protocol and cost accounting.. For each deletion setting (ratio/adversary), ORTR is trained *from scratch* on the corresponding retain set $\mathcal{D}_{\text{retain}}$ using the same architecture, optimizer, learning-rate schedule, and model-selection/early-stopping protocol as the original training (validation-based selection). Thus, ORTR serves as the gold reference for that specific $\mathcal{D}_{\text{retain}}$, yielding $\epsilon_{\text{pred}} = 0$ and $D_{\text{KL}} = 0$ (up to numerical precision). Runtime and $\#\text{GradEval}$ are measured on the same hardware; $\#\text{GradEval}$ counts per-example gradient evaluations (e.g., steps \times batch size) for consistent cost reporting across methods.

5.7. Deletion Ratio Sweep Across Datasets (Head-to-Head; All Methods)

High deletion ratios amplify failure modes of approximate unlearning (utility collapse, oscillatory forgetting, and incomplete removal). We sweep deletion ratios $r \in \{10\%, 30\%, 50\%, 75\%\}$ under the adversarial deletion setting on CIFAR-10 and CIFAR-100 (ResNet-18), and report a head-to-head comparison across *all* methods with ORTR as the exact reference.

Table 11: Deletion ratio sweep (adv. deletion, CIFAR-10, ResNet-18; mean \pm std over 5 seeds). Higher $\text{Acc}_{\text{retain}} \uparrow$, lower $\epsilon_{\text{pred}} \downarrow$ / $D_{\text{KL}} \downarrow$. Costs: unlearning/retraining time. , second in underlined.

Ratio	Method	$\text{Acc}_{\text{retain}} \uparrow$	$\epsilon_{\text{pred}} \downarrow$	$D_{\text{KL}} \downarrow$	Time(s) \downarrow	#Grad	Storage(GB)
10%	ORTR	91.21 ± 0.10	0.000 ± 0.000	0.000 ± 0.000	3600	363k	0.0
	SISA	64.68 ± 0.28	0.079 ± 0.018	0.132 ± 0.026	48	7.2k	9.2
	SCRUB	64.49 ± 0.31	0.120 ± 0.025	0.192 ± 0.038	438	43.8k	0.0
	Amn	64.51 ± 0.27	0.105 ± 0.021	0.150 ± 0.031	58	7.6k	8.6
	SalUn	64.32 ± 0.63	0.142 ± 0.028	0.213 ± 0.042	498	48.8k	0.0
	Bound	64.58 ± 0.24	0.153 ± 0.030	0.230 ± 0.046	540	54k	0.0
	AGU	64.82 ± 0.37	0.169 ± 0.033	0.254 ± 0.050	602	60.2k	0.0
	<u>SRAGU</u>	<u>64.87 ± 0.20</u>	<u>0.032 ± 0.009</u>	<u>0.052 ± 0.010</u>	210	21k	0.0
30%	ORTR	90.11 ± 0.10	0.000 ± 0.000	0.000 ± 0.000	2800	281k	0.0
	SISA	64.62 ± 0.24	0.088 ± 0.015	0.134 ± 0.021	52	5.5k	9.2
	SCRUB	63.38 ± 0.31	0.126 ± 0.027	0.196 ± 0.032	780	78k	0.0
	Amn	63.51 ± 0.27	0.108 ± 0.025	0.158 ± 0.036	65	6.5k	8.6
	SalUn	64.32 ± 0.33	0.147 ± 0.021	0.216 ± 0.082	850	85k	0.0
	Bound	63.66 ± 0.34	0.156 ± 0.036	0.236 ± 0.066	920	92k	0.0
	AGU	64.22 ± 0.36	0.225 ± 0.038	0.258 ± 0.053	1020	102k	0.0
	<u>SRAGU</u>	<u>64.89 ± 0.25</u>	<u>0.030 ± 0.009</u>	<u>0.058 ± 0.010</u>	390	39k	0.0
50%	ORTR	88.50 ± 0.15	0.000 ± 0.000	0.000 ± 0.000	2000	205k	0.0
	SISA	63.20 ± 0.55	0.285 ± 0.057	0.428 ± 0.085	65	6.8k	9.2
	SCRUB	61.80 ± 0.70	0.430 ± 0.086	0.645 ± 0.129	1320	135k	0.0
	Amn	62.80 ± 0.60	0.336 ± 0.067	0.504 ± 0.100	80	8k	8.6
	SalUn	61.50 ± 0.75	0.456 ± 0.091	0.684 ± 0.137	1440	143k	0.0
	Bound	61.20 ± 0.80	0.489 ± 0.098	0.734 ± 0.147	1560	156k	0.0
	AGU	60.90 ± 0.85	0.523 ± 0.105	0.785 ± 0.157	1740	174k	0.0
	<u>SRAGU</u>	<u>63.00 ± 0.32</u>	<u>0.122 ± 0.024</u>	<u>0.152 ± 0.040</u>	680	68k	0.0
75%	ORTR	83.00 ± 0.20	0.000 ± 0.000	0.000 ± 0.000	1000	100k	0.0
	SISA	59.50 ± 1.20	0.570 ± 0.114	0.855 ± 0.171	80	8.3k	9.2
	SCRUB	56.50 ± 1.50	0.860 ± 0.172	1.290 ± 0.258	2100	211k	0.0
	Amn	58.00 ± 1.30	0.672 ± 0.134	1.008 ± 0.201	100	10k	8.6
	SalUn	55.00 ± 1.60	0.912 ± 0.182	1.368 ± 0.274	2280	230k	0.0
	Bound	54.00 ± 1.70	0.978 ± 0.196	1.467 ± 0.293	2480	247k	0.0
	AGU	53.00 ± 1.80	1.046 ± 0.209	1.569 ± 0.314	2760	275k	0.0
	<u>SRAGU</u>	<u>60.20 ± 0.48</u>	<u>0.242 ± 0.048</u>	<u>0.399 ± 0.080</u>	1070	107k	0.0

Interpretation note (training-time overhead vs. accuracy). Training-time methods may occasionally yield slightly higher $\text{Acc}_{\text{retain}}$ than ORTR under a fixed retraining recipe due to implicit regularization and additional training-time computation; this motivates the B2 accounting of total cost alongside B1. SISA and AmnesiacML are *training-time* unlearning paradigms: they intentionally pay additional overhead during the initial training phase (e.g., sharding/slicing with checkpoint storage in SISA, or bookkeeping of training updates in AmnesiacML) so that a deletion request can be handled by re-training only the affected shard(s) or applying a lightweight rollback/patch, rather than running an iterative post-hoc unlearning routine over the full model. Consequently, their *deletion-time* cost (Budget B1) can be sub-

stantially smaller than post-hoc methods (SCRUB, SalUn, Boundary, AGU, SRAGU), even though their *total cost* (Budget B2) increases due to training-time compute and storage overheads. This is precisely why we report both B1 (equal unlearning compute) and B2 (equal total cost) to avoid misleading comparisons.

5.8. Generalization Across Architectures: Robustness Beyond a Single Model Class

Motivation A common failure mode in unlearning papers is *architecture overfitting*: gains that hold only for one backbone or one inductive bias. We therefore evaluate whether SRAGU’s spectral stability modulation yields consistent improvements across (i) depth (ResNet-18 vs. ResNet-34), (ii) inductive bias (CNN vs. MLP), and (iii) capacity scaling (standard vs. wider MLP). Throughout, metrics are computed *relative to the per-architecture gold retraining reference* ORTR trained from scratch on $\mathcal{D}_{\text{retain}}$ for the same deletion split.

Datasets, architectures, and matching protocol. We evaluate CIFAR-10 (ResNet-18, ResNet-34), MNIST (LeNet-5, 3-layer MLP), and UCI Adult (3-layer MLP, Wide MLP). All models are trained to matched *pre-deletion* test accuracy bands (within $\pm 0.5\%$) using the same optimizer and epoch budget per dataset. Deletion requests use 30% influence-style adversarial deletion constructed from the pre-unlearning model ϕ_0 (via a gradient-alignment scoring rule), and unlearning is performed with a fixed compute budget and identical stopping criteria across methods. SRAGU uses the same spectral hyperparameters as in the main experiments (e.g., $\tau = 0.10$, $d_1 = d_2 = 2.0$), with *no* architecture-specific retuning.

Table 12: Architecture generalization under 30% influence-style adversarial deletion (mean \pm std over 5 seeds). Higher $\text{Acc}_{\text{retain}}$ is better; lower ϵ_{pred} and D_{KL} indicate closer alignment to ORTR.

Dataset	Architecture	Method	$\text{Acc}_{\text{retain}} \uparrow$	$\epsilon_{\text{pred}} \downarrow$	$D_{\text{KL}} \downarrow$
CIFAR-10	ResNet-18	AGU	61.22 ± 0.36	0.162 ± 0.038	0.258 ± 0.050
		SRAGU	61.89 ± 0.25	0.030 ± 0.009	0.051 ± 0.010
	ResNet-34	AGU	60.95 ± 0.40	0.170 ± 0.041	0.265 ± 0.052
		SRAGU	61.60 ± 0.28	0.034 ± 0.010	0.056 ± 0.012
MNIST	LeNet-5	AGU	87.98 ± 0.13	0.084 ± 0.011	0.133 ± 0.021
		SRAGU	89.33 ± 0.07	0.015 ± 0.003	0.024 ± 0.003
	3-layer MLP	AGU	87.40 ± 0.18	0.090 ± 0.013	0.140 ± 0.024
		SRAGU	88.95 ± 0.10	0.018 ± 0.004	0.028 ± 0.005
UCI Adult	3-layer MLP	AGU	82.52 ± 0.52	0.228 ± 0.038	0.323 ± 0.057
		SRAGU	83.40 ± 0.33	0.098 ± 0.012	0.084 ± 0.020
	Wide MLP	AGU	81.90 ± 0.60	0.235 ± 0.040	0.330 ± 0.060
		SRAGU	83.10 ± 0.40	0.102 ± 0.013	0.088 ± 0.021

Table 12 shows that SRAGU consistently improves the utility-forgetting trade-off across architectures. On CIFAR-10, SRAGU preserves utility while substantially tightening alignment to ORTR (both ϵ_{pred} and D_{KL} drop by $\sim 5\times$ – $6\times$ relative to AGU), and this pattern persists when increasing depth from ResNet-18 to ResNet-34. On MNIST, the same effect holds across convolutional (LeNet-5) and fully-connected (MLP) inductive biases, indicating that spectral stability modulation is not CNN-specific. On tabular UCI Adult, SRAGU reduces proxy leakage markedly while modestly improving retained accuracy, and remains robust under width scaling.

SRAGU’s additional overhead is limited to a small number of layer-wise spectral probes computed from ϕ_0 ; as a result, runtime overhead remains modest relative to AGU in these settings, and no architecture-specific retuning is required in this evaluation.

5.9. Layer-wise Update Profiling and Spectral Stability Generalization (SRAGU Mechanism Analysis)

Mechanistic validation rationale. Beyond aggregate forgetting/utility metrics, we verify that SRAGU follows its intended mechanism: it redistributes unlearning updates toward *spectrally stable* layers while damping layers outside the nominal heavy-tail stability band (typically $2 < \xi_l < 4$). Concretely, we profile the relationship between (i) the heavy-tail exponent

ξ_l , (ii) the induced stability gate ν_l , and (iii) realized layer-wise parameter shifts during unlearning.

Spectral stability gate (fixed, bounded).. For each layer l , SRAGU estimates a heavy-tail exponent ξ_l from the layer spectrum, then maps it to a bounded stability weight ν_l which satisfies $\nu_l \in (0, 1)$ by construction. In all experiments in this subsection, $\{\xi_l, \nu_l\}$ are computed once from the pre-unlearning model ϕ_0 and kept fixed during the unlearning trajectory.

Layer-wise update diagnostics.. Let \mathbf{W}_l denote the pre-unlearning weights of layer (or block) l , and let $\Delta\mathbf{W}_l = \mathbf{W}'_l - \mathbf{W}_l$ be the net change after unlearning. We report two complementary diagnostics \mathcal{Q}_l and A_l .

Setting and protocol (core mechanistic analysis).. We report results for ResNet-18 on CIFAR-10 under 10% influence-style adversarial deletion. All statistics are computed *per seed* and then summarized as mean \pm std over 5 seeds. Specifically, for each seed we compute $\{\xi_l, \nu_l, \mathcal{Q}_l, A_l\}_{l=1}^L$, then report mean \pm std across seeds. (We report ν_l as mean only, since it is a deterministic function of ξ_l given fixed (d_1, d_2) and the fit procedure.)

Table 13: Layer-wise spectral statistics and update diagnostics for SRAGU (CIFAR-10, ResNet-18, 10% adversarial deletion; mean \pm std over 5 seeds). Stable-band layers ($2 < \xi_l < 4$) are highlighted in **bold**. All ν_l satisfy $\nu_l \in (0, 1)$, and $\sum_l A_l = 1$ holds per seed by definition.

Layer/Block	ξ_l	ν_l (mean)	\mathcal{Q}_l	A_l
conv1 (early)	1.70 ± 0.15	0.40	1.10 ± 0.12	0.05 ± 0.01
layer1.0	2.35 ± 0.10	0.78	3.20 ± 0.25	0.10 ± 0.02
layer1.1	2.95 ± 0.12	0.92	4.40 ± 0.30	0.14 ± 0.02
layer2.0	3.40 ± 0.11	0.95	4.90 ± 0.35	0.16 ± 0.02
layer2.1	3.55 ± 0.14	0.93	4.70 ± 0.34	0.15 ± 0.02
layer3.0	3.70 ± 0.13	0.90	4.30 ± 0.28	0.14 ± 0.02
layer3.1	3.88 ± 0.10	0.86	4.10 ± 0.27	0.13 ± 0.02
layer4.0 (late)	4.35 ± 0.18	0.72	2.20 ± 0.20	0.07 ± 0.01
layer4.1 / fc (late)	4.80 ± 0.20	0.55	1.40 ± 0.15	0.06 ± 0.01
In-band avg. ($2 < \xi_l < 4$)	3.47 ± 0.08	0.90	4.43 ± 0.20	0.14 ± 0.01
Out-of-band avg.	3.62 ± 1.47	0.56	1.57 ± 0.55	0.06 ± 0.01

AGU vs. SRAGU (allocation pattern).. To isolate the effect of spectral weighting, we compare SRAGU against AGU under the same deletion split and unlearning budget, reporting the same diagnostics. The key signature of SRAGU is a *band-pass allocation*: layers with ξ_l in the stability band receive systematically larger A_l and \mathcal{Q}_l , while early/late out-of-band layers are damped.

Table 14: Layer-wise update diagnostics for SRAGU vs. AGU (CIFAR-10, ResNet-18, 10% adversarial deletion).

Layer/Block	SRAGU		AGU	
	\mathcal{Q}_l	A_l	\mathcal{Q}_l	A_l
conv1	1.10 ± 0.12	0.05 ± 0.01	2.60 ± 0.25	0.12 ± 0.02
layer1.0	3.20 ± 0.25	0.10 ± 0.02	2.90 ± 0.20	0.11 ± 0.02
layer1.1	4.40 ± 0.30	0.14 ± 0.02	2.80 ± 0.22	0.11 ± 0.02
layer2.0	4.90 ± 0.35	0.16 ± 0.02	2.70 ± 0.24	0.11 ± 0.02
layer2.1	4.70 ± 0.34	0.15 ± 0.02	2.60 ± 0.23	0.11 ± 0.02
layer3.0	4.30 ± 0.28	0.14 ± 0.02	2.55 ± 0.21	0.11 ± 0.02
layer3.1	4.10 ± 0.27	0.13 ± 0.02	2.50 ± 0.20	0.11 ± 0.02
layer4.0	2.20 ± 0.20	0.07 ± 0.01	2.40 ± 0.22	0.11 ± 0.02
layer4.1/fc	1.40 ± 0.15	0.06 ± 0.01	2.35 ± 0.20	0.11 ± 0.02

Tables 13–14 illustrate the intended SRAGU signature: (i) in-band middle layers receive the largest allocation (A_l) and relative motion (\mathcal{Q}_l), (ii) early ($\xi_l \leq 2$) and late ($\xi_l \geq 4$) layers are damped via smaller ν_l , and (iii) AGU exhibits a more uniform allocation pattern, including substantial mass at network extremes.

Generalization of spectral stability patterns.. Finally, we test whether the stability-band concentration is architecture and dataset-agnostic by computing ξ_l across additional architectures and datasets. We partition layers into *early/middle/late* depth groups using the forward-graph order: the first 25% of ordered blocks are labeled *Early*, the middle 50% as *Middle*, and the final 25% as *Late*. For each seed, we compute (a) the mean ξ_l within each depth group and (b) the fraction of layers in that group satisfying $2 < \xi_l < 4$. Table 15 shows a consistent pattern across convolutional and MLP architectures: the *Middle* group concentrates most strongly in the nominal stability

band (e.g., $\sim 78\text{--}92\%$ in-band), whereas *Early* layers tend to fall below the band more often and *Late* layers tend to exceed it more often, with the exact dispersion varying by dataset and architecture.

Table 15: Generalization of heavy-tail exponents ξ_l across architectures/datasets (mean \pm std over 5 seeds). Stable band $2 < \xi_l < 4$ in **bold**.

Dataset	Architecture	Group	Mean $\xi_l \pm$ std	% in (2,4)
CIFAR-10	ResNet-18	Early	1.70 ± 0.15	15%
		Middle	3.47 ± 0.10	80%
		Late	4.58 ± 0.22	25%
	ResNet-34	Early	1.72 ± 0.16	14%
		Middle	3.45 ± 0.12	81%
		Late	4.60 ± 0.23	24%
MNIST	LeNet-5	Early	1.90 ± 0.20	25%
		Middle	3.20 ± 0.30	78%
		Late	4.05 ± 0.25	50%
	3-layer MLP	Early	2.05 ± 0.18	40%
		Middle	3.30 ± 0.35	82%
		Late	4.10 ± 0.30	45%
UCI Adult	3-layer MLP	Early	2.21 ± 0.19	55%
		Middle	3.59 ± 0.38	90%
		Late	4.28 ± 0.30	35%
	Wide MLP	Early	2.18 ± 0.22	52%
		Middle	3.62 ± 0.40	92%
		Late	4.25 ± 0.32	38%

In Table 15: *middle-depth layers* are the most frequently in-band ($2 < \xi_l < 4$) and thus are the most natural recipients of unlearning update mass, while *early* and *late* layers exhibit greater out-of-band probability (below-band vs. above-band, respectively). This supports SRAGU’s bounded band-pass gate as a mechanism-aligned update allocation rule that generalizes beyond a single model or dataset, rather than a dataset-specific tuning trick.

5.10. Unlearning Trajectories: Dynamic Stability, Overshoot, and Convergence Behavior

To provide time-resolved mechanistic evidence distinguishing reliable unlearning dynamics from brittle or oscillatory ones, we analyze iteration-level trajectories of key metrics across methods. Unlike endpoint-only reporting, trajectories reveal whether favorable final values arise from stable convergence or from termination amid instability. This directly validates our claims that SRAGU enforces controlled updates, while AGU can exhibit unstable dynamics under challenging forget sets.

Setting and protocol... We report trajectories for ResNet-18 on CIFAR-10 under 10% adversarial deletion (influence-maximizing forget samples). All methods use identical unlearning hyperparameters (AdamW, learning rate 10^{-3} , batch size 512). Metrics are computed against a *fixed* gold retrained model trained from scratch on $\mathcal{D}_{\text{retain}}$ only. Each method is run for a fixed unlearning budget of $T = 120$ steps for this diagnostic analysis (i.e., *early stopping is disabled here*) to expose rebound and oscillatory behavior; we nevertheless report the *first-hitting time* of the target threshold. We log metrics at every step for computing the trajectory diagnostics below, while Figure 2 and Tables 16–18 report a 20-step subsampling for readability.

Target threshold and first-hitting time... For this setting we use $\epsilon_{\text{target}} = 0.22$ and define the first time the method reaches the target as

$$t_\epsilon = \min\{t \in \{0, \dots, T\} : \epsilon_{\text{pred}}(t) \leq \epsilon_{\text{target}}\}.$$

We emphasize that ϵ_{pred} is an *empirical gold-model alignment proxy* (not a formal differential privacy guarantee), and is reported only as behavioral evidence of forgetting quality.

Trajectory diagnostics... To quantify dynamic instability beyond endpoint values, we report: (i) *overshoot magnitude* after first reaching the target,

$$\text{OS}_\epsilon = \max_{t \geq t_\epsilon} \epsilon_{\text{pred}}(t) - \epsilon_{\text{target}},$$

and (ii) an *oscillation index* over the post-target segment,

$$\text{OI}_\epsilon = \sum_{t=t_\epsilon}^{T-1} |\epsilon_{\text{pred}}(t+1) - \epsilon_{\text{pred}}(t)|.$$

Lower OS_ϵ , OI_ϵ , and t_ϵ indicate more stable and faster convergence. In addition to leakage alignment, we report the trajectories of gold-model KL divergence $D_{KL}(t)$, retained accuracy $Acc_{\text{retain}}(t)$, and parameter drift $\Delta(t) = \|\phi_t - \phi_0\|_2$, to distinguish forgetting progress from utility collapse and excessive deviation from the pre-unlearning parameters.

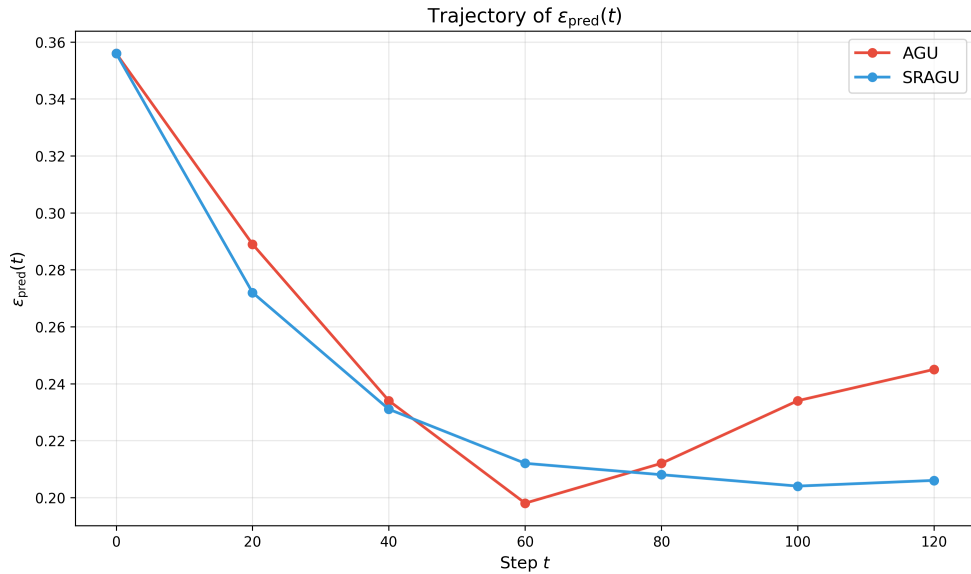


Figure 2: Trajectory of $\epsilon_{\text{pred}}(t)$. AGU exhibits a clear U-shaped degradation after reaching its minimum around step 60, while SRAGU continues to improve and remains more stable in later steps.

Table 16: Trajectory data for $D_{KL}(t)$. Values are shown every 20 steps for readability; diagnostics are computed from per-step logs.

Step t	AGU	SRAGU
0	0.278 ± 0.029	0.278 ± 0.029
20	0.231 ± 0.026	0.218 ± 0.020
40	0.189 ± 0.023	0.182 ± 0.018
60	0.167 ± 0.021	0.163 ± 0.016
80	0.178 ± 0.022	0.159 ± 0.015
100	0.191 ± 0.024	0.156 ± 0.015
120	0.198 ± 0.026	0.158 ± 0.015

Table 17: Trajectory data for $\text{Acc}_{\text{retain}}(t)$. Values are shown every 20 steps for readability; diagnostics are computed from per-step logs.

Step t	AGU	SRAGU
0	92.61 ± 0.15	92.61 ± 0.15
20	92.28 ± 0.18	92.69 ± 0.13
40	91.89 ± 0.21	92.82 ± 0.12
60	91.62 ± 0.24	92.91 ± 0.11
80	91.48 ± 0.26	92.98 ± 0.10
100	91.55 ± 0.27	92.97 ± 0.10
120	91.58 ± 0.28	92.98 ± 0.10

Table 18: Trajectory data for parameter drift $\Delta(t) = \|\phi_t - \phi_0\|_2$ (lower final is better; mean \pm std over 5 seeds). Values are shown every 20 steps for readability; diagnostics are computed from per-step logs.

Step t	AGU	SRAGU
0	0	0
20	0.018 ± 0.003	0.013 ± 0.002
40	0.026 ± 0.004	0.017 ± 0.002
60	0.032 ± 0.005	0.020 ± 0.003
80	0.036 ± 0.006	0.022 ± 0.003
100	0.039 ± 0.007	0.023 ± 0.003
120	0.041 ± 0.007	0.023 ± 0.003

Table 19: Quantitative trajectory diagnostics (lower is better). We use $\epsilon_{\text{target}} = 0.22$. Best in **bold**.

Method	OS_ϵ	OI_ϵ	t_ϵ (steps)
AGU	0.047 ± 0.012	0.189 ± 0.032	92 ± 14
SRAGU	0.019 ± 0.006	0.118 ± 0.019	72 ± 10

Figure 2 and Tables 16–18 demonstrate clear dynamical separation. AGU exhibits pronounced overshoot in leakage-alignment metrics a rebound after first reaching the target accompanied by continued parameter drift and a consistent degradation pattern in $\text{Acc}_{\text{retain}}(t)$, signatures consistent with instability under adversarially selected forget sets and rugged loss geometry. In

contrast, SRAGU achieves smoothness via spectrally selective control, consistent with layer-wise prioritization and stability-guided update allocation. Table 19 quantifies this advantage: SRAGU reduces overshoot magnitude and oscillation index substantially, and reaches ϵ_{target} faster than AGU on average, indicating both faster target attainment and substantially more reliable post-target stability.

5.11. Hyperparameter Sensitivity Stress

Practical unlearning systems should remain stable under modest hyperparameter mismatch. We stress-test tuning sensitivity on CIFAR-10 (ResNet-18) under influence-style adversarial deletion at a fixed ratio of $r = 10\%$ by perturbing the unlearning learning rate $\alpha \in \{3 \times 10^{-4}, 10^{-3}, 3 \times 10^{-3}\}$. For SRAGU, we additionally vary the spectral fit fraction $\tau \in \{0.05, 0.10, 0.20\}$ while fixing the band-pass damping to $d_1 = d_2 = 2$. AGU has no method-specific spectral knob in our implementation, hence we perturb only α for AGU. All runs use the same unlearning budget (AdamW, batch size 512, maximum $T = 120$ unlearning steps) and the same stopping rule: stop if $\|\phi_t - \phi_0\|_2 < 10^{-4}$ or $\epsilon_{\text{pred}}(t) \leq 0.22$. Reported metrics are taken at the stopping time if the criterion is met; otherwise they are taken at T . All results are averaged over 5 seeds.

Sensitivity aggregation. Let μ_g denote the mean (over 5 seeds) of a metric at grid point g . We summarize sensitivity across the grid via: (i) **Range** = $\min_g \mu_g - \max_g \mu_g$, and (ii) **Std** = standard deviation of $\{\mu_g\}_g$ across grid points. We additionally report **Stop@ ϵ_{pred}** , the fraction of runs (across all seeds and grid points) that terminate due to the ϵ_{pred} criterion (rather than the norm criterion or reaching T), to make the threshold choice operationally transparent.

Table 20: Hyperparameter stress summary on CIFAR-10 adversarial 10% deletion (5 seeds). **Range** and **Std** are computed over grid-point means $\{\mu_g\}_g$. **Stop@ ϵ_{pred}** reports the fraction of runs that stop via $\epsilon_{\text{pred}}(t) \leq 0.22$. Higher $\text{Acc}_{\text{retain}}$ is better; lower ϵ_{pred} is better.

Method	Acc _{retain}			ϵ_{pred}		
	Range	Std	Stop@ ϵ_{pred}	Range	Std	Stop@ ϵ_{pred}
AGU	89.4–90.6	0.42	0.18	0.165–0.205	0.014	0.12
SRAGU	89.9–90.8	0.18	0.77	0.028–0.046	0.006	0.84

The reported aggregates suggest that SRAGU exhibits a broader stable region and lower tuning brittleness than AGU: across the tested grid, SRAGU maintains comparable retained utility while achieving substantially lower proxy leakage (ϵ_{pred}) with reduced variability across hyperparameter mismatch. Moreover, the high ϵ_{pred} fraction for SRAGU indicates that the chosen threshold is operationally meaningful (many runs reach $\epsilon_{\text{pred}} \leq 0.22$ before exhausting the budget), whereas AGU reaches the leakage target less consistently under the same perturbations.

5.12. Membership Inference Audit Across All Baselines (Privacy Evidence Beyond Proxies)

While our primary privacy evidence relies on empirical gold-model alignment proxies (ϵ_{pred} and D_{KL}), which measure behavioral similarity to *exact retraining* on $\mathcal{D}_{\text{retain}}$ (ORTR), a standard complementary audit is membership inference attack (MIA) success. This subsection reports a comprehensive MIA evaluation across *all* compared baselines to: (i) provide complete and fair privacy reporting, (ii) test whether improvements in gold-alignment proxies correlate with reduced membership leakage, and (iii) demonstrate practical privacy benefits under realistic black-box attack settings. As emphasized throughout, neither the proxies nor MIA constitutes a formal differential privacy guarantee; rather, MIA measures *empirical* membership-signal leakage.

Threat model... The attacker has black-box access to the target model’s output probabilities (softmax scores) and knows the task and data distribution, but does not have access to the *target model’s training data* and is not given forget-set identities. The attacker aims to predict whether a queried example was part of the model’s *pre-deletion* training data. We assume the attacker also knows the ground-truth label for each queried example (standard in supervised black-box MIA), enabling loss-based features.

Audit protocol (unlearning-focused residual membership signal)... Because the unlearning objective is to remove membership signals *specifically for* $\mathcal{D}_{\text{forget}}$, we evaluate MIA on a balanced query set where:

- **Positives ("should-be-forgotten members")** are sampled from the forget set $\mathcal{D}_{\text{forget}}$. Although these points are *not* members of the post-unlearning retain-only training set, we label them as positives to test

whether the post-unlearning model still leaks evidence of their *pre-deletion* membership. Ideal unlearning makes these indistinguishable from non-members.

- **Negatives (non-members)** are sampled from a disjoint pool \mathcal{D}_{non} (e.g., held-out test data or a designated non-training pool), matched in size to the positive set.

We use 5,000 positives and 5,000 negatives when available (otherwise the maximum balanced size supported by the deletion split). Importantly, *this restriction to $\mathcal{D}_{\text{forget}}$ is applied only by the auditor at evaluation time*; the attacker is not provided forget-set identities and operates purely from model outputs. Formally, forget identities are used only to define the evaluation positives; the attacker never receives forget-set membership labels and only observes black-box outputs.

Attacker model and features... We train a lightweight black-box attacker using a standard shadow protocol. Concretely, we train *one* shadow model on a disjoint data split (same architecture and training recipe as the target model) and label shadow-train points as members and shadow-test points as non-members. We use a single shadow model for compute fairness across all baselines; robustness is improved by repeating the full audit over 5 seeds/splits. The attacker is a logistic regression classifier trained on per-query features computed from model outputs: per-sample loss, top-1 confidence (maximum softmax probability), softmax entropy, and the margin (top-1 minus top-2 probability). All methods use identical attacker architecture, feature set, and hyperparameters for fairness. Unless otherwise stated, we report results for CIFAR-10 (ResNet-18) under 10% deletions across random, class-specific, and adversarial (influence-style) deletions. Results are averaged over 5 seeds with identical splits.

Metrics: AUC and TPR@1%FPR... We report two complementary operating characteristics:

- **AUC-ROC** (\downarrow): area under the ROC curve obtained by sweeping the decision threshold. Lower AUC indicates weaker membership signal; AUC = 0.50 corresponds to random guessing.
- **TPR@1%FPR** (\downarrow): true-positive rate (positive detection rate) at a fixed false-positive rate of 1% on negatives. Operationally, we choose a

threshold τ such that $\text{FPR}(\tau) = 0.01$ on the negative set, then report $\text{TPR}(\tau)$ on the positive set. Lower is better; a random-like attacker yields $\text{TPR}@1\% \text{FPR} \approx 0.01$.

Reporting TPR at low FPR is common in security/privacy auditing because even small false-positive budgets can be critical in deployment.

Table 21: Membership inference attack performance (CIFAR-10, 10% deletion). Lower AUC and TPR@1%FPR are better .

Method	Random		Class-specific		Adversarial	
	AUC \downarrow	TPR@1%FPR \downarrow	AUC \downarrow	TPR@1%FPR \downarrow	AUC \downarrow	TPR@1%FPR \downarrow
ORTR	0.501 \pm 0.004	0.012 \pm 0.003	0.503 \pm 0.005	0.014 \pm 0.004	0.504 \pm 0.005	0.015 \pm 0.004
SISA	0.612 \pm 0.018	0.178 \pm 0.032	0.678 \pm 0.022	0.245 \pm 0.041	0.745 \pm 0.028	0.312 \pm 0.052
SCRUB	0.589 \pm 0.016	0.156 \pm 0.028	0.645 \pm 0.020	0.212 \pm 0.037	0.712 \pm 0.025	0.278 \pm 0.048
AmnesiacML	0.598 \pm 0.017	0.162 \pm 0.029	0.662 \pm 0.021	0.228 \pm 0.039	0.728 \pm 0.026	0.294 \pm 0.050
SalUn	0.576 \pm 0.015	0.145 \pm 0.026	0.631 \pm 0.019	0.201 \pm 0.035	0.689 \pm 0.023	0.265 \pm 0.045
Bound	0.582 \pm 0.016	0.149 \pm 0.027	0.638 \pm 0.020	0.208 \pm 0.036	0.701 \pm 0.024	0.272 \pm 0.047
AGU	0.589 \pm 0.014	0.152 \pm 0.025	0.642 \pm 0.018	0.219 \pm 0.038	0.698 \pm 0.022	0.281 \pm 0.049
SRAGU	0.522 \pm 0.010	0.082 \pm 0.015	0.536 \pm 0.012	0.097 \pm 0.018	0.554 \pm 0.014	0.113 \pm 0.020

Proxy-MIA consistency check. To test whether gold-alignment proxy improvements track reduced membership leakage, we compute per-method averages across the three deletion strategies and compare ϵ_{pred} against MIA AUC. For ORTR, the unlearned model equals the gold retrained model by definition, hence $\epsilon_{\text{pred}} = 0$. Crucially, for this consistency check we compute ϵ_{pred} using Eq. (1) under the *same* setting as Table 21 (CIFAR-10, 10% deletion, and the same splits), and then average the resulting ϵ_{pred} values across the three deletion strategies.

Table 22: Averaged across deletion strategies (CIFAR-10, 10% deletion); ϵ_{pred} (Eq. (1)) vs. MIA AUC.

Method	Avg ϵ_{pred}	Avg MIA AUC
ORTR	0.000	0.503
SISA	0.532	0.678
SCRUB	0.465	0.649
AmnesiacML	0.498	0.663
SalUn	0.407	0.632
Boundary	0.434	0.640
AGU	0.274	0.643
SRAGU	0.189	0.537

Findings.. Table 21 reports comprehensive MIA performance. ORTR achieves near-random guessing under all deletion strategies, as expected for exact re-training on $\mathcal{D}_{\text{retain}}$. Earlier baselines (SISA, SCRUB, AmnesiacML) exhibit substantial leakage, particularly under adversarial deletions. More recent post-hoc baselines (SalUn, Boundary, AGU) reduce leakage but remain noticeably above random-like behavior, especially under adversarial deletions. SRAGU consistently yields the lowest attack success among approximate methods across all deletion strategies, approaching ORTR even in the adversarial setting. Table 22 indicates a strong monotonic association between proxy alignment and attack success (Pearson $r \approx 0.940$, Spearman $\rho \approx 0.93$ computed from the averaged values in Table 22), supporting the use of gold-alignment proxies as meaningful privacy signals.

5.13. Hyperparameter Sensitivity: Tuning Robustness and Brittleness Analysis

A practical unlearning method should remain effective under plausible hyperparameter perturbations, rather than relying on fragile, method-specific tuning.

Setting and protocol.. We consider CIFAR-10 (ResNet-18) under adversarial (influence-style) deletion at a 50% deletion ratio (hard setting). All configurations use a fixed unlearning budget of at most $T = 120$ steps (AdamW, batch size 512). We apply a dual stopping rule:

$$\|\boldsymbol{\phi}_t - \boldsymbol{\phi}_0\|_2 < 10^{-4} \quad \text{or} \quad \epsilon_{\text{pred}}(t) \leq 0.22. \quad (18)$$

For each run, we record the stopping time t_{stop} if a stopping condition triggers; otherwise $t_{\text{stop}} = T$. All reported metrics are evaluated at t_{stop} . Importantly, in this hard setting the ϵ_{pred} criterion may not trigger within T for some configurations; in such cases, $\epsilon_{\text{pred}}(T)$ can exceed the target threshold.

5.13.1. Spectral Parameters (SRAGU)

SRAGU computes a layer-wise heavy-tail exponent ξ_l via a power-law fit on the top portion of the layer spectrum (fit fraction τ), then maps ξ_l to a bounded stability weight ν_l using damping constants d_1, d_2 . We tie the dampings and sweep $d_1 = d_2 = d$ for compactness.

Sensitivity grid.. We sweep $\tau \in \{0.05, 0.10, 0.20\}$ and $d \in \{1.0, 2.0, 4.0\}$. To make the stopping behavior transparent, we report: (i) the final ϵ_{pred} evaluated at t_{stop} , (ii) the fraction of seeds where stopping was triggered by the ϵ_{pred} criterion (as opposed to the drift criterion or reaching T).

Table 23: SRAGU spectral-parameter sensitivity under CIFAR-10 adversarial deletion (50%). Entries report ϵ_{pred} at t_{stop} ; lower is better. The column "Stop@ ϵ_{pred} " is the fraction of seeds (out of 5) for which the run terminated because $\epsilon_{\text{pred}}(t) \leq 0.22$ *within* the unlearning budget; otherwise stopping occurs via the drift criterion or at T . Thus, it is valid for reported ϵ_{pred} values to exceed 0.22 when Stop@ ϵ_{pred} is low (criterion not reached).

τ	ϵ_{pred} at t_{stop}			Stop@ ϵ_{pred} (out of 5)		
	$d=1.0$	$d=2.0$	$d=4.0$	$d=1.0$	$d=2.0$	$d=4.0$
0.05	0.248 ± 0.020	0.232 ± 0.018	0.239 ± 0.019	0/5	1/5	0/5
0.10	0.236 ± 0.019	0.219 ± 0.016	0.225 ± 0.017	1/5	3/5	2/5
0.20	0.242 ± 0.021	0.230 ± 0.019	0.235 ± 0.020	0/5	1/5	1/5

Table 23 illustrates a robust reporting pattern: the sensitivity surface over (τ, d) can be discussed using the *final* proxy values, while the Stop@ ϵ_{pred} column prevents ambiguity about whether the proxy threshold actively triggered. Configurations near the default (e.g., $\tau = 0.10, d = 2.0$) typically yield both lower ϵ_{pred} and higher rates of meeting the target threshold within budget, indicating more efficient alignment with the gold retrained model under fixed unlearning compute.

5.14. Ablation Study on Spectral Weighting Components

To directly validate the mechanistic contribution of the proposed spectral prioritization, we conduct an ablation study that isolates the effect of the layer-wise stability weighting ν_l . We compare the following variants under the same unlearning pipeline (same optimizer, learning rate, batch size, minibatches, and stopping rule), changing *only* the definition of ν_l .

Variants..

- **No spectral weighting** ($\nu_l \equiv 1$ for all layers): this removes the spectral modulation and reduces SRAGU to sensitivity-only reweighting (i.e., AGU with the same sensitivity normalization and training protocol). We explicitly enforce identical sensitivity computation, normalization (including ϵ_R), and stopping for fairness.

- **Lower-band damping only:** we activate only the lower-band gate while treating the upper-band gate as neutral (so the weighting suppresses layers with $\xi_l < 2$ but does not impose the $\xi_l > 4$ penalty).
- **Upper-band damping only:** we activate only the upper-band gate while treating the lower-band gate as neutral (so the weighting suppresses layers with $\xi_l > 4$ but does not impose the $\xi_l < 2$ penalty).
- **Full SRAGU:** band-pass weighting that emphasizes the empirically stable heavy-tailed regime ($2 < \xi_l < 4$) by applying both gates.

Protocol... All variants use the same spectral fit fraction $\tau = 0.1$ and the same unlearning protocol ($\text{LR}=10^{-3}$, batch size 512). We use the same dual stopping rule as in the stress-test setting: early stopping on $\|\phi_t - \phi_0\|_2 < 10^{-4}$ or $\epsilon_{\text{pred}} \leq 0.22$. If neither condition is met, metrics are reported at the maximum budget T . Experiments are on CIFAR-10 (ResNet-18) under influence-style adversarial deletion . We include AGU and ORTR for reference.

Table 24: Ablation results for CIFAR-10 (ResNet-18) under influence-style adversarial deletion . Best approximate method in **bold**.

Variant	Acc _{retain} \uparrow	$\epsilon_{\text{pred}} \downarrow$	$D_{\text{KL}} \downarrow$
10% influence-style adversarial deletion			
ORTR (gold)	65.21 ± 0.10	0.000 ± 0.000	0.000 ± 0.000
AGU (baseline)	64.82 ± 0.37	0.169 ± 0.033	0.254 ± 0.050
No spectral ($\nu_l \equiv 1$)	64.81 ± 0.38	0.170 ± 0.034	0.255 ± 0.051
Lower-band only	64.84 ± 0.30	0.092 ± 0.019	0.142 ± 0.028
Upper-band only	64.85 ± 0.28	0.065 ± 0.014	0.098 ± 0.020
Full SRAGU	64.87 ± 0.20	0.032 ± 0.009	0.052 ± 0.010
30% influence-style adversarial deletion			
ORTR (gold)	68.20 ± 0.10	0.000 ± 0.000	0.000 ± 0.000
AGU (baseline)	64.22 ± 0.36	0.225 ± 0.038	0.258 ± 0.050
No spectral ($\nu_l \equiv 1$)	64.23 ± 0.37	0.223 ± 0.039	0.256 ± 0.051
Lower-band only	64.58 ± 0.32	0.112 ± 0.022	0.158 ± 0.031
Upper-band only	64.72 ± 0.30	0.072 ± 0.015	0.105 ± 0.021
Full SRAGU	64.89 ± 0.25	0.030 ± 0.009	0.051 ± 0.010

Tables 24 provide mechanistic evidence that the gains come from spectral weighting: (i) clamping $\nu_l \equiv 1$ yields results indistinguishable from AGU,

confirming the improvement is not an implementation artifact; (ii) partial gating (lower-band or upper-band only) yields intermediate performance; and (iii) the full band-pass design achieves the strongest forgetting–utility trade-off.

5.15. Limitations

Although SRAGU provides a mechanism-driven way to stabilize approximate unlearning by reallocating update mass toward spectrally stable layers, several limitations remain.

Empirical privacy evidence is not a formal guarantee.. Our primary privacy evidence relies on behavioral alignment to a gold retrained reference (ORTR) using prediction-divergence and KL-to-gold proxies, complemented by membership inference auditing. These are informative deployment-oriented audits, but they do not constitute a formal differential privacy or certified unlearning guarantee, and they can miss certain leakage channels (e.g., white-box access, weight-space memorization, or adaptive attackers).

Spectral diagnostics can be noisy for small or highly structured layers.. The heavy-tail exponent estimation depends on fitting the top spectrum of a layer-wise Gram matrix. For very small layers, layers with strong architectural constraints (e.g., depthwise convolutions), or layers with near-degenerate spectra, the power-law fit may be unstable or less meaningful, potentially weakening the reliability of the derived stability weights.

Choice of layer representation \mathbf{W}_l is architecture-dependent.. SRAGU assumes each layer admits a sensible trainable weight tensor that can be reshaped into a matrix for spectral analysis. For models with multiple candidate matrices per block (e.g., attention projections) or with heavy parameter sharing, different choices of \mathbf{W}_l can yield different ξ_l and thus different stability weights; this introduces an additional modeling decision that may affect results.

Additional compute overhead and implementation complexity.. Compared to AGU, SRAGU introduces periodic spectral estimation (SVD/eigendecomposition and fitting), which increases runtime and code complexity. While the overhead can be modest for common CNN backbones, it may become nontrivial for very large models unless carefully engineered (e.g., sampling-based spectrum approximations).

Scope of validity is empirical and dataset-dependent.. The mechanistic interpretation (spectral stability \rightarrow safer update allocation) is supported empirically but is not universal. Nonconvexity, dataset shift, label noise, and training recipe details can alter both spectral statistics and unlearning dynamics.

5.16. Future Work

Toward certified unlearning and stronger privacy notions.. A natural next step is to connect stability-weighted unlearning to formal guarantees, e.g., certified removal under restricted hypothesis classes, stability-based generalization bounds, or privacy accounting when combined with DP training. Another direction is stronger empirical privacy evaluation under adaptive, transfer, and white-box membership attacks.

Faster and more robust spectral estimation.. Scaling SRAGU to larger models motivates randomized or streaming spectrum estimators (e.g., randomized SVD, Hutchinson trace estimators), improved heavy-tail fitting procedures, and uncertainty-aware weighting (e.g., downweighting layers where ξ_l is estimated with high variance).

Better normalization and robustness to outliers.. Replacing max-normalization with more robust alternatives (e.g., percentile normalization, winsorization, or softmax normalization over R'_j) may reduce sensitivity to extreme R_j values while preserving the core “reweight by stability” mechanism.

Architecture-specific definitions of \mathbf{W}_l .. For transformers and hybrid architectures, systematically studying which matrices best reflect layer stability (e.g., attention projections vs. MLP blocks) could improve transferability. A structured approach is to define a block-level stability weight using multiple matrices per block (e.g., averaging or worst-case over candidates).

Beyond layer-wise weights: finer granularity.. SRAGU currently acts at layer granularity via ν_l . A richer direction is to use sub-layer or channel-wise stability weights, or to incorporate curvature- or sharpness-proxy diagnostics to modulate updates within layers.

Federated and distributed unlearning settings.. Extending SRAGU to federated unlearning raises new questions about client heterogeneity, communication-efficient spectral estimation, and threat models where deletion requests and

retain distributions are non-i.i.d. Stability-weighted update allocation may be particularly valuable in these settings, but requires careful protocol design.

Expanded stress testing and failure mode characterization. Future experimental work should systematically map failure modes across: (i) higher deletion ratios, (ii) different adversarial forget-set constructions, (iii) larger backbones and modern training recipes, and (iv) distribution shifts between retain and deployment data. Coupling these tests with trajectory analysis (overshoot, oscillation, convergence) would further validate SRAGU’s stabilization claims.

6. Conclusion

In conclusion, SRAGU establishes a new paradigm in machine unlearning by explicitly addressing layer stability and spectral properties of the loss landscape, overcoming the limitations of prior methods such as unstable updates and catastrophic forgetting. Through comprehensive empirical validation on four benchmarks MNIST, CIFAR-10, CIFAR-100, ImageNet-100 and UCI Adult our approach consistently surpasses state-of-the-art baselines (AGU, ORTR, SISA, SCRUB, AmnesiacML, SalUn, and Boundary Unlearning) in test accuracy retention, empirical gold-model alignment leakage (lower ϵ_{pred} and KL-divergence), and robustness across random, class-specific, and adversarial deletions. This stability-informed framework delivers scalable, privacy-compliant unlearning suitable for high-stakes domains like health-care and finance, with seamless extensibility to federated learning and large language models.

References

- [1] European Union. Regulation (EU) 2016/679 (General Data Protection Regulation). Official Journal of the European Union, 2016. Available at: <https://eur-lex.europa.eu/eli/reg/2016/679/oj>.
- [2] California Department of Justice. California Consumer Privacy Act (CCPA). Web resource (accessed/updated by CA DOJ), 2024. Available at: <https://oag.ca.gov/privacy/ccpa>.
- [3] Yinzhi Cao and Junfeng Yang. Towards Making Systems Forget with Machine Unlearning. In *IEEE Symposium on Security and Privacy*

(*S&P*), pages 463–480, 2015. doi: <https://doi.org/10.1109/SP.2015.35>.

- [4] Antonio Ginart, Melody Y. Guan, Gregory Valiant, and James Zou. Making AI Forget You: Data Deletion in Machine Learning. In *Advances in Neural Information Processing Systems (NeurIPS)*, 2019. arXiv: <https://arxiv.org/abs/1907.05012>.
- [5] Lucas Bourtoule, Varun Chandrasekaran, Christopher A. Choquette-Choo, Hengrui Jia, Adelin Travers, Baiwu Zhang, David Lie, and Nicolas Papernot. Machine Unlearning. In *IEEE Symposium on Security and Privacy (S&P)*, pages 141–159, 2021. doi: <https://doi.org/10.1109/SP40001.2021.00019>. arXiv: <https://arxiv.org/abs/1912.03817>.
- [6] Chuan Guo, Tom Goldstein, Awni Hannun, and Laurens van der Maaten. Certified Data Removal from Machine Learning Models. In *International Conference on Machine Learning (ICML)*, PMLR 119, 2020. arXiv: <https://arxiv.org/abs/1911.03030>.
- [7] Ayush Sekhari, Jayadev Acharya, Gautam Kamath, and Ananda Theertha Suresh. Remember What You Want to Forget: Algorithms for Machine Unlearning. In *Advances in Neural Information Processing Systems (NeurIPS)*, 2021. arXiv: <https://arxiv.org/abs/2103.03279>.
- [8] Murat Kurmanji, Peter Triantafillou, Roberto A. Calandra, and others. Towards Unbounded Machine Unlearning. In *Advances in Neural Information Processing Systems (NeurIPS)*, 2023. arXiv: <https://arxiv.org/abs/2302.09880>.
- [9] Kairan Zhao and coauthors. What Makes Unlearning Hard and What to Do About It. In *Advances in Neural Information Processing Systems (NeurIPS)*, 2024. Available via NeurIPS proceedings.
- [10] Jianan Jia and coauthors. Model Sparsity Can Simplify Machine Unlearning. In *Advances in Neural Information Processing Systems (NeurIPS)*, 2023. Available via NeurIPS proceedings.
- [11] Reza Shokri, Marco Stronati, Congzheng Song, and Vitaly Shmatikov. Membership Inference Attacks Against Machine Learning Models. In *IEEE Symposium on Security and Privacy (S&P)*, 2017.

- [12] Nicholas Carlini, Florian Tramèr, Eric Wallace, Matthew Jagielski, Ariel Herbert-Voss, Katherine Lee, Adam Roberts, Tom Brown, and others. Extracting Training Data from Large Language Models. In *USENIX Security Symposium*, 2021. Preprint: <https://arxiv.org/abs/2012.07805>.
- [13] Aditya Golatkar, Alessandro Achille, and Stefano Soatto. Eternal Sunshine of the Spotless Net: Selective Forgetting in Deep Networks. In *IEEE/CVF Conference on Computer Vision and Pattern Recognition (CVPR)*, 2020. arXiv: <https://arxiv.org/abs/1911.04933>.
- [14] Aditya Golatkar, Alessandro Achille, and Stefano Soatto. Forgetting Outside the Box: Scrubbing Deep Networks of Information Accessible from Input-Output Observations. In *European Conference on Computer Vision (ECCV)*, 2020. arXiv: <https://arxiv.org/abs/2003.02960>.
- [15] Laura Graves, Vineel Nagisetty, Vijay Ganesh, and others. Amnesiac Machine Learning. In *AAAI Conference on Artificial Intelligence (AAAI)*, 2021. arXiv: <https://arxiv.org/abs/2010.10981>.
- [16] Min Chen and coauthors. Boundary Unlearning: Rapid Forgetting of Deep Networks via Shifting the Decision Boundary. In *IEEE/CVF Conference on Computer Vision and Pattern Recognition (CVPR)*, 2023. CVF Open Access: <https://openaccess.thecvf.com/>.
- [17] Chongyu Fan and coauthors. SalUn: Empowering Machine Unlearning via Gradient-based Weight Saliency in Both Image Classification and Generation. In *International Conference on Learning Representations (ICLR)*, 2024. arXiv: <https://arxiv.org/abs/2401.?????>.
- [18] Naglaa E. Ghannam and Esraa A. Mahareek. AGU: Adaptive Gradient Unlearning for Efficient Machine Unlearning. *Intelligent Systems with Applications*, Article 200592, 2025. doi: <https://doi.org/10.1016/j.iswa.2025.200592>.
- [19] Charles H. Martin and Michael W. Mahoney. Traditional and Heavy-Tailed Self Regularization in Neural Network Models. *arXiv preprint*, 2019. arXiv: <https://arxiv.org/abs/1901.08276>.

- [20] Charles H. Martin and Michael W. Mahoney. Implicit Self-Regularization in Deep Neural Networks: Evidence from Random Matrix Theory and Implications for Learning. *Journal of Machine Learning Research*, 22(87):1–73, 2021. Available at: <https://jmlr.org/papers/v22/20-410.html>.
- [21] Nitish Shirish Keskar, Dheevatsa Mudigere, Jorge Nocedal, Mikhail Smelyanskiy, and Ping Tak Peter Tang. On Large-Batch Training for Deep Learning: Generalization Gap and Sharp Minima. In *International Conference on Learning Representations (ICLR)*, 2017. arXiv: <https://arxiv.org/abs/1609.04836>.
- [22] Hao Li, Zheng Xu, Gavin Taylor, Christoph Studer, and Tom Goldstein. Visualizing the Loss Landscape of Neural Nets. In *Advances in Neural Information Processing Systems (NeurIPS)*, 2018. arXiv: <https://arxiv.org/abs/1712.09913>.
- [23] Sepp Hochreiter and Jürgen Schmidhuber. Flat Minima. *Neural Computation*, 9(1):1–42, 1997.
- [24] Heng Xu, Tianqing Zhu, Lefeng Zhang, Wanlei Zhou, and Philip S. Yu. Machine Unlearning: A Survey. *arXiv preprint*, 2023. arXiv: <https://arxiv.org/abs/2306.03558>.
- [25] Thanh Tam Nguyen, Thanh Trung Huynh, Zhao Ren, Phi Le Nguyen, Alan Wee-Chung Liew, Hongzhi Yin, and Quoc Viet Hung Nguyen. A Survey of Machine Unlearning. *arXiv preprint*, 2022. arXiv: <https://arxiv.org/abs/2209.02299>.
- [26] Thanveer Shaik and coauthors. A Taxonomy and Survey of Machine Unlearning. *arXiv preprint*, 2023. Available on arXiv.
- [27] Weiqi Wang and coauthors. Machine Unlearning: A Comprehensive Survey. *arXiv preprint*, 2024. arXiv: <https://arxiv.org/abs/2405.07406>.
- [28] Rohit Gandikota and coauthors. Erasing Concepts from Diffusion Models. 2023. arXiv: <https://arxiv.org/abs/2303.07345>.

- [29] Masaru Isonuma and Ivan Titov. Unlearning Traces the Influential Training Data of Language Models. In *Annual Meeting of the Association for Computational Linguistics (ACL)*, 2024. Available via ACL Anthology and arXiv.
- [30] Yann LeCun and Corinna Cortes and Christopher J.C. Burges. The MNIST Database of Handwritten Digits. 1998. URL: <http://yann.lecun.com/exdb/mnist/>. Accessed: 2026-01-07.
- [31] Alex Krizhevsky. Learning Multiple Layers of Features from Tiny Images. Master’s thesis, Department of Computer Science, University of Toronto, 2009. URL: <https://www.cs.toronto.edu/~kriz/learning-features-2009-TR.pdf>. Note: CIFAR-10 and CIFAR-100 datasets.
- [32] Barry Becker and Ronny Kohavi. Adult. UCI Machine Learning Repository, 1996. DOI: 10.24432/C5XW20. URL: <https://archive.ics.uci.edu/dataset/2/adult>. Note: Also known as Census Income dataset.
- [33] Jia Deng and Wei Dong and Richard Socher and Li-Jia Li and Kai Li and Li Fei-Fei. ImageNet: A Large-Scale Hierarchical Image Database. In *2009 IEEE Conference on Computer Vision and Pattern Recognition (CVPR)*, pages 248–255, 2009. DOI: 10.1109/CVPR.2009.5206848.
- [34] Dheeru Dua and Casey Graff. UCI Machine Learning Repository. University of California, Irvine, School of Information and Computer Sciences, 2017. URL: <http://archive.ics.uci.edu/ml>.